Eur. J. Mech. B - Fluids 19 (2000) 37–68

The effect of wall cooling on compressible Görtler vortices

John W. Elliott [a,*], Andrew P. Bassom [b,1]

[a] *Department of Mathematics, University of Hull, Hull HU6 7RX, UK*
[b] *School of Mathematical Sciences, University of Exeter, North Park Road, Exeter, Devon EX4 4QE, UK*

(Received 10 December 1998; revised 20 April 1999; accepted 29 July 1999)

Abstract – It is known that in adiabatic boundary layer flow over a curved surface the detailed structure of the spanwise periodic Görtler vortex instability varies markedly over the range of spanwise wavelength. At short wavelengths the modes tend to be concentrated in a well-defined thin zone located within the boundary layer. As the vortex wavenumber diminishes so the region of vortex activity is first driven to the bounding wall but subsequently expands to cover the entire boundary layer at which stage the modes take on a principally inviscid form. At yet longer wavelengths the vortices are given by the solution of an interactive multi-deck structure which has some similarities with that for Tollmien–Schlichting waves.

In this work we investigate how the application of wall cooling affects the above scenario. It is shown how cooling both restricts the range of mode types and gives rise to two new structures. The first, for moderate cooling and which relates to longer wavelengths, is interactive in nature. Here the viscous–inviscid interaction between an essentially inviscid Görtler problem, albeit for an effective basic flow which in its general form has a non-standard near-wall structure, and a viscous sublayer is provided by novel boundary conditions. Shorter wavelength vortices are largely unaffected by wall cooling unless this is quite severe. However when this degree of cooling is applied, the vortices take on a fully viscous form and are confined to a thin region next to the bounding wall wherein the basic flow assumes an analytic form. Numerical solutions are obtained and we provide evidence as to how the two new structures are related both to each other and to the previously known uncooled results. © 2000 Éditions scientifiques et médicales Elsevier SAS

compressible Görtler vortex / Tollmien–Schlichting waves

1. Introduction

Following the pioneering study by Görtler [1] into spanwise periodic vortex instability, which can manifest itself in boundary layer flow over slightly concave surfaces, there have been numerous investigations into this centrifugally-driven mechanism. The relevant stability equations for the Görtler vortex mode take the form of a parabolic partial differential system which can be solved numerically by straightforward marching in the downstream direction. Hall [2] has shown that the quantitative details of the spatial development of Görtler flow is sensitive to non-parallel effects: a conclusion that carries over to compressible flows as well [3]. An important implication of these results is that the concept of a unique, linear neutral stability curve, which is so familiar in many hydrodynamical contexts, does not exist for the Görtler problem. In general, for modes with wavelength comparable with the boundary layer thickness, the downstream neutral locations are entirely dependent on how and where the disturbance initiated so that different starting conditions yield different 'neutral curves'. The one exception to this behaviour occurs in the high-Görtler, high-wavenumber regime for which Hall [4] was able to demonstrate that nonparallelism is less important and so unique growth-rate curves can be determined. Subsequently there have been numerous papers on the subject and for a full account of progress the reader is referred to suitable review papers, e.g., Hall [5] or Saric [6]. Most investigations have, for simplicity,

* Correspondence and reprints; j.w.elliott@maths.hull.ac.uk
[1] drew@maths.exeter.ac.uk

concentrated on the case of two-dimensional incompressible boundary layers although it is recognised that in nature many situations in which Görtler vortices arise the flow will be three-dimensional and compressible.

The spectrum of Görtler modes is discrete and at large Görtler numbers G (see (1) below) there is a whole hierarchy of possible modes. These take on a layered structure, with the number of layers increasing with the mode number. For a given two-dimensional boundary layer the growth-rate curve relating to some given initial vortex structure has two neutral points. That is, in an experimental setting a vortex imposed at some specified streamwise location typically decays over a certain distance, then passes through a region of amplification before final decay sets in. For large values $G \gg 1$ the right-hand side of the linear neutral curve moves to a vortex wavenumber $k = \mathrm{O}(G^{1/4})$ (here the vortex wavelength is expressed relative to the local boundary layer thickness). Hall [4] elucidated the structure pertaining to this right-hand branch and Timoshin [7] and Denier, Hall and Seddougui [8] later identified a second viscous structure which captures the mode with the greatest spatial growth rate: in this regime $k = \mathrm{O}(G^{1/5})$. At O(1) wavelengths the vortices take on a principally inviscid form and occupy the whole of the boundary layer. Hall and Malik [9] and Dando and Seddougui [10] studied the compressible counterparts to the right-hand branch and most unstable structures and the latter authors also uncovered a second mode: this is trapped in the thin temperature adjustment layer which forms within a compressible boundary layer at sufficiently large Mach numbers. Rozhko and Ruban [11] demonstrated that as the mode wavenumber falls so an interactive viscous–inviscid mechanism increasingly comes into play. This process, which can be thought of as the large spanwise wavelength limit of a Tollmien–Schlichting wave, is described by a triple-deck formulation and was exploited by Rozhko and Ruban [11] to examine disturbances generated by streamwise elongated roughness elements over curved surfaces (see also Ruban [12] and Rozhko, Ruban and Timoshin [13]). Choudhari, Hall and Streett [14], hereafter referred to as CHS, also used this triple-deck both to investigate flows over humps and, as the vortex wavelength increases further, to show that the interactive structure gives way to one in which Görtler modes become fully non-parallel and amenable only to an entirely numerical treatment (Hall [2], Bogolepov and Lipatov [15], CHS [14]). In total the five regimes corresponding to (i) the right-hand branch; (ii) the most amplified mode; (iii) inviscid vortices; (iv) the viscous–inviscid interactive mechanism and (v) non-parallel modes encompass the possibilities for Görtler vortices across the entire wavenumber range. By way of summary, and for future reference, the schematic *figure 1* shows the locations of these five modes in parameter space (denoted I–V respectively) and records their associated spatial growth rates.

The main emphasis in this paper is on an investigation into the effects of wall cooling on the Görtler structure. Wall cooling is employed in many physical situations, principally because high-speed flows generate extreme heat and artificial cooling is often needed to keep surfaces at reasonable working temperatures. Most investigations concerned with the effects of wall-cooling upon boundary-layer stability have concentrated on its effects upon inviscid shear modes. Initially it was assumed that cooling should stabilise matters, as it causes the disappearance of the inflexion point associated with the so-called second mode which, in general, constitutes the most unstable mode at higher Mach numbers. However recent studies, for example Mack [16] and Shaw and Duck [17], have criticised this conclusion, since no account seems to have been made to quantify the effect of cooling upon the higher inviscid modes. Shaw and Duck [17] indicate that while cooling stabilises the lowest inviscid mode it destabilises the others—a conclusion that has been confirmed by El Hady [18] who also proved that cooling tends to stabilise secondary instabilities.

The influence of wall cooling on viscous modes has thus far only been investigated in the context of compressible Tollmien–Schlichting waves, that is the ‘first mode’ of instability. Seddougui, Bowles and Smith [19] demonstrated that cooling destabilises the flow to the extent that the enhanced viscous growth rates rival those of the usually larger inviscid ones: see also Brown et al. [20] and Kerimbekov et al. [21]. Given the important role cooling often plays in practical situations, it is perhaps surprising that very little work (both

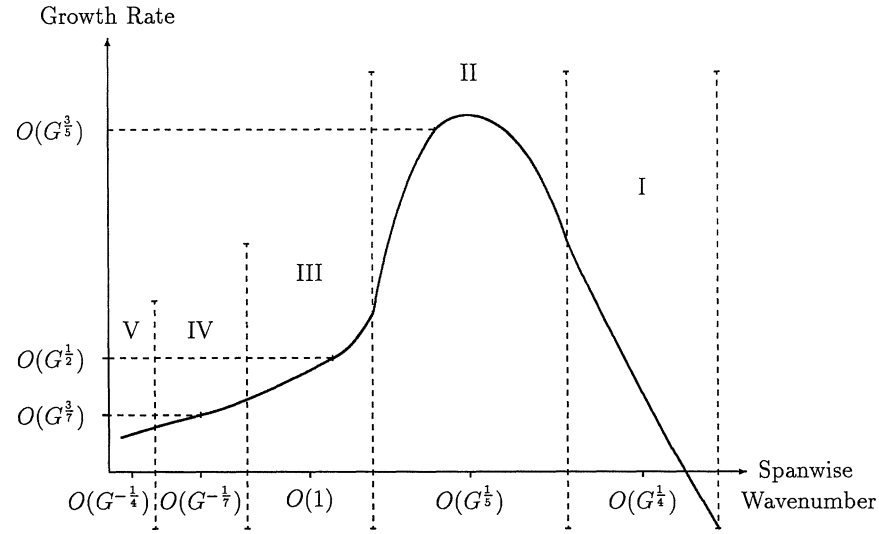

Figure 1. Schematic showing the wavenumber regimes and associated spatial amplification rates for the five principal forms of Görtler modes within an incompressible boundary layer. Regions I–V correspond to the right-hand branch, the most amplified regime, the inviscid modes, the domain of the interactive structure of Choudhari et al. [14] and the fully non-parallel modes respectively.

theoretical and experimental) seems to have been done concerning its influence with regards to Görtler vortices. El Hady and Verma [22] considered the linear Görtler instability of a low Mach number flow and suggested that unless the cooling is quite marked it has little effect although significant cooling tends to be stabilising. In contrast, Hall and Fu [23] examined the structure of Görtler vortices at hypersonic speeds and in later work (Fu and Hall [24,25]) suggested that the application of wall cooling makes the temperature adjustment layer, wherein the modes are trapped, increasingly unstable to Rayleigh instability. More recently, Bogolepov [26] looked at the properties of stationary cooled inviscid vortices in hypersonic flow and concluded that cooling tends to be destabilising.

In order to improve our understanding of the role of cooling for Görtler modes, the study outlined here contains both analytical and numerical work which reveals a number of links between the previously known uncooled structures and some new configurations: we endeavour to clarify these as we proceed. In order to highlight the part played by cooling as opposed to other factors we shall, like many previous authors, restrict ourselves to a two-dimensional basic flow although the generalisation to three dimensions is in many cases quite straightforward. Our starting point is with the comprehensive study by Dando and Seddougui [10] of inviscid Görtler vortices and we show how limited cooling modifies their results. The influence of cooling on the viscous–inviscid long wavelength structure summarised in CHS [14] is also considered and we show that cooling leads to significant alterations in the nature of the vortices. Indeed, for sufficient cooling (the precise magnitude of which is specified in due course) a novel ‘moderately cooled’ interactive mode arises. This effectively combines both the above uncooled modes in as much that the corresponding numerical problem reduces to solving for a cooled inviscid vortex coupled to the solution of a viscous sublayer via the inner boundary conditions. As the degree of cooling is increased further a second new mode is discovered and we find that this form can also be obtained by taking appropriate limits of each of the structures I–III shown in *figure 1*. Hereafter we shall refer to this mode as being ‘severely cooled’ and its properties are found to be determined after the numerical solution of some viscous equations.

The remainder of the paper is organised as follows. In Section 2 we set out the governing equations and do so within a fairly general setting. We undertake a study of some of the properties of the basic flow and follow this,

in Section 3, with a quick review of Dando and Seddougui's [10] inviscid work, but with some cooling included. The parallel question as to the effect of cooling on the long-wavelength interactive structure of CHS [14] is tackled in Section 4 where we also develop the properties of the new moderately cooled interactive modes referred to above. Numerical solutions of the associated inviscid stability equation are pursued in Section 5. Next, in Section 6, it is shown how further cooling leads to the identification of the second novel form (the viscous 'severely cooled' structure) and the relationships between this and the modes I–III of *figure 1* are clarified. The salient determining equations for the severely cooled modes are derived and some numerical solutions of these are described. The paper closes with some discussion of the findings and points the way towards possible extensions of our work.

2. The general problem

Let us take a boundary layer flowing over a curved surface $\bar{y} = 0,\ -\infty < \bar{z} < \infty$ with the axes oriented such that the x-coordinate denotes distance along the curved surface while $\bar{y}$ measures the distance normal to it. If $\bar{z}$ denotes the spanwise co-ordinate let us suppose that the surface has variable curvature $\chi(x)/b$. In this formulation the co-ordinates $(x, \bar{y}, \bar{z})$, the time t and the corresponding velocity components $(\tilde{u}, \bar{v}, \bar{w})$ have been made dimensionless with respect to $l_\infty,\ l_\infty/U_\infty$ and U_∞, where l_∞ and U_∞ denote a characteristic lengthscale and free-stream velocity in the streamwise direction. (We notice that the two key streamwise lengthscales b and l_∞ need not coincide.) Finally, we define $\rho_\infty\widetilde{\rho},\ T_\infty\widetilde{T},\ \mu_\infty\widetilde{\mu}$ and $\rho_\infty U_\infty^2\widetilde{p}$ to be the density, temperature, viscosity and pressure of the fluid, where the subscript ∞ has been used to denote typical free-stream values. The Reynolds number *Re*, Görtler number G and free-stream Mach number M_∞ are defined according to

$$Re = \frac{\rho_\infty U_\infty l_\infty}{\mu_\infty}, \qquad G = 2\frac{l_\infty}{b}Re^{1/2}, \qquad M_\infty = \frac{U_\infty}{a_\infty}, \tag{1}$$

where $a_\infty = \gamma p_\infty/\rho_\infty$ is the free-stream speed of sound and γ is the ratio of specific heats. In the case of large Reynolds number we introduce the usual boundary-layer scalings $(\bar{y}, \bar{z}, \bar{v}, \bar{w}) = \mathrm{Re}^{-1/2}(y, z, \tilde{v}, \tilde{w})$ and write the pressure in the form

$$\widetilde{p} = \frac{1}{\gamma M_\infty^2}\pi_B(x) + \frac{1}{Re}\widetilde{P}(x, y, z).$$

The resulting compressible boundary-layer equations for the two-dimensional basic flow need to be supplemented by the equation of state for a perfect gas $\widetilde{\rho}\widetilde{T} = \pi_B$ and a suitable viscosity-temperature law. For simplicity here we opt for Chapman's law[2] $\widetilde{\mu} = C\widetilde{T}$: we also assume that $\Delta = \widetilde{\lambda}/\widetilde{\mu}$, the ratio of the first and second coefficients of viscosity, is constant. The compressible boundary-layer equations for the basic flow then need to be solved subject to the wall conditions

$$\widetilde{u} = \widetilde{v} = 0, \quad \widetilde{T} = T_w \quad \text{at } y = 0$$

and the free-stream requirements

$$\widetilde{u} \to U_e(x), \quad \widetilde{T} \to T_e(x) \equiv 1 + \frac{1}{2}(\gamma - 1)M_\infty^2(1 - U_e^2) \quad \text{as } y \to \infty,$$

[2] In related studies we have also conducted the entire analysis for a general power law in which $\widetilde{\mu} \propto \widetilde{T}^n$: details are available from either author on request.

where we have assumed the outer flow is homoentropic.

The general form of the relevant stability equations may be obtained by substituting a flow of the form

$$(\widetilde{u}, \widetilde{v}, \widetilde{w}, \widetilde{P}, \widetilde{\rho}, \widetilde{T}, \widetilde{\mu}) = (U_B, V_B, 0, P_B, R_B, T_B, \mu_B) + \delta(u, v, w, P, \rho, T, \mu) + \mathrm{O}(\delta^2) \tag{2}$$

into the compressible Navier–Stokes equations. Here the parameter $\delta \ll 1$ measures the amplitude of the vortex and the quantities with subscript B denote basic flow entities. With the expressions (2) the linearised versions of the stability equations can be written

$$R_B\left(\frac{\partial u}{\partial x} + \frac{\partial v}{\partial y} + \frac{\partial w}{\partial z}\right) + \rho\left(\frac{\partial U_B}{\partial x} + \frac{\partial V_B}{\partial y}\right) + \left(\frac{\partial}{\partial t} + U_B\frac{\partial}{\partial x} + V_B\frac{\partial}{\partial y}\right)\rho + \left(u\frac{\partial R_B}{\partial x} + v\frac{\partial R_B}{\partial y}\right) = 0, \tag{3a}$$

$$R_B\left\{\left(\frac{\partial}{\partial t} + U_B\frac{\partial}{\partial x} + V_B\frac{\partial}{\partial y}\right)u + \left(u\frac{\partial U_B}{\partial x} + v\frac{\partial U_B}{\partial y}\right)\right\} + \rho\left(U_B\frac{\partial U_B}{\partial x} + V_B\frac{\partial U_B}{\partial y}\right) = \frac{\partial}{\partial y}\left(\mu_B\frac{\partial u}{\partial y} + \mu\frac{\partial U_B}{\partial y}\right) + \frac{\partial}{\partial z}\left(\mu_B\frac{\partial u}{\partial z}\right), \tag{3b}$$

$$R_B\left\{\left(\frac{\partial}{\partial t} + U_B\frac{\partial}{\partial x} + V_B\frac{\partial}{\partial y}\right)v + \left(u\frac{\partial V_B}{\partial x} + v\frac{\partial V_B}{\partial y}\right) + G\chi U_B u\right\} + \rho\left(U_B\frac{\partial V_B}{\partial x} + V_B\frac{\partial V_B}{\partial y} + \frac{1}{2}G\chi U_B^2\right) = -\frac{\partial P}{\partial y} + \frac{\partial}{\partial y}\left(\mu_B\frac{\partial v}{\partial y} + \mu\frac{\partial V_B}{\partial y}\right) + \frac{\partial}{\partial z}\left(\mu_B\frac{\partial v}{\partial z}\right) + \Delta\frac{\partial}{\partial y}\left[\mu_B\left(\frac{\partial u}{\partial x} + \frac{\partial v}{\partial y} + \frac{\partial w}{\partial z}\right) + \mu\left(\frac{\partial U_B}{\partial x} + \frac{\partial V_B}{\partial y}\right)\right] + \frac{\partial}{\partial x}\left(\mu_B\frac{\partial u}{\partial y} + \mu\frac{\partial U_B}{\partial y}\right) + \frac{\partial}{\partial y}\left(\mu_B\frac{\partial v}{\partial y} + \mu\frac{\partial V_B}{\partial y}\right) + \frac{\partial}{\partial z}\left(\mu_B\frac{\partial w}{\partial y}\right), \tag{3c}$$

$$R_B\left(\frac{\partial}{\partial t} + U_B\frac{\partial}{\partial x} + V_B\frac{\partial}{\partial y}\right)w = -\frac{\partial P}{\partial z} + \frac{\partial}{\partial y}\left(\mu_B\frac{\partial w}{\partial y}\right) + \frac{\partial}{\partial z}\left(\mu_B\frac{\partial w}{\partial z}\right) + \Delta\frac{\partial}{\partial z}\left[\mu_B\left(\frac{\partial u}{\partial x} + \frac{\partial v}{\partial y} + \frac{\partial w}{\partial z}\right) + \mu\left(\frac{\partial U_B}{\partial x} + \frac{\partial V_B}{\partial y}\right)\right] + \frac{\partial}{\partial x}\left(\mu_B\frac{\partial u}{\partial z}\right) + \frac{\partial}{\partial y}\left(\mu_B\frac{\partial v}{\partial z}\right) + \frac{\partial}{\partial z}\left(\mu_B\frac{\partial w}{\partial z}\right), \tag{3d}$$

$$R_B\left\{\left(\frac{\partial}{\partial t} + U_B\frac{\partial}{\partial x} + V_B\frac{\partial}{\partial y}\right)T + \left(u\frac{\partial T_B}{\partial x} + v\frac{\partial T_B}{\partial y}\right)\right\} - \frac{(\gamma-1)}{\gamma}u\frac{d\pi_B}{dx} + \rho\left(U_B\frac{\partial T_B}{\partial x} + V_B\frac{\partial T_B}{\partial y}\right) = \frac{1}{\sigma}\left\{\frac{\partial}{\partial y}\left(\mu_B\frac{\partial T}{\partial y} + \mu\frac{\partial T_B}{\partial y}\right) + \frac{\partial}{\partial z}\left(\mu_B\frac{\partial T}{\partial z}\right)\right\} + (\gamma-1)M_\infty^2\left[2\mu_B\frac{\partial U_B}{\partial y}\frac{\partial u}{\partial y} + \mu\left(\frac{\partial U_B}{\partial y}\right)^2\right]. \tag{3e}$$

In these equations σ denotes the Prandtl number of the fluid and we remark that in all the subsequent calculations we set $\sigma = 1$ and the ratio of specific heats $\gamma = 1.4$.

The continuity, momentum and energy balances (3) need to be supplemented by the appropriate linearisations of the state and Chapman law equations

$$R_B T + \rho T_B = 0, \tag{3f}$$

$$\mu = CT, \tag{3g}$$

where the basic flow quantities satisfy $R_B T_B = \pi_B,\ \mu_B = C T_B$. Finally, the system (3a)–(3g) is subject to the homogeneous conditions

$$u = v = w = T = 0 \quad \text{at } y = 0 \text{ and as } y \to \infty. \tag{4}$$

The above problem, save with the viscosity form (3g) replaced by Sutherland's law, was tackled by Wadey [3] in order to investigate the evolution of vortices in compressible flows.

In what follows we shall assume that the Görtler number $G \gg 1$ and that the vortex perturbations take the form

$$(u, v, w, P) \propto \exp(\beta x + ikz - i\Omega t), \tag{5}$$

where $\beta,\ k$ and Ω are the growth rate, spanwise wavenumber and frequency respectively. The condition for the problem to be essentially parallel (that is, for non-parallelism to play only a secondary role) is that $\beta \gg 1$. The complicated natures of some of the structures below means that it is almost inevitable that some notation has to be given a number of roles within the paper. The alternative would be to introduce a plethora of obscure variable names that would make the account more difficult to follow. Thus some variables will be re-defined from section to section: in addition we adopt the convention that any variables based on k or β will be (loosely) referred to as spanwise vortex wavenumber and growth rate respectively.

2.1. The basic flow

Before we can embark on a study of the vortices, we need to comment upon the important properties of the basic flow. We remark that in what follows it is sometimes easier to proceed in terms of the co-ordinate y and at other points better to use the Dorodnitsyn variable η defined by $\eta = \int_0^y dy/T_B$—we shall freely change between the two without special comment.

When written in terms of the Dorodnitsyn variable the governing equations for the basic flow take the form

$$U_B = \frac{\partial \psi}{\partial \eta}, \tag{6a}$$

$$\frac{\pi_B}{T_B}\left[\frac{\partial \psi}{\partial \eta}\frac{\partial^2 \psi}{\partial \eta \partial x} - \frac{\partial \psi}{\partial x}\frac{\partial^2 \psi}{\partial \eta^2}\right] = \left(U_e \frac{dU_e}{dx}\right)\frac{\pi_B}{T_e} + \frac{C}{T_B}\frac{\partial^3 \psi}{\partial \eta^3}. \tag{6b}$$

Without loss of generality we may take the constant $C = 1$ in the viscosity law for its value can always be adjusted using a suitable re-scaling of η. For simplicity we shall assume the absence of a pressure gradient and take $\pi_B = U_e = 1$ for which a straightforward similarity solution exists. If $U_B = f'(\widehat{\eta}),\ T_B = T_B(\widehat{\eta})$ is taken, where $\widehat{\eta} \equiv \eta x^{-1/2}$, then we have Blasius' equation $f''' + (1/2) f f'' = 0$ subject to $f(0) = f'(0) = 0$, $f'(\infty) = 1$: here primes denote differentiation with respect to $\widehat{\eta}$. Note that for this special case $f(\widehat{\eta})$ is

independent of the temperature field.[3] For Prandtl number $\sigma = 1$ the temperature is then given by

$$T_B = T_w + \left[(T_r - T_w) f' - (T_r - 1)(f')^2\right], \tag{7}$$

where $T_e = 1$ and $T_r = 1 + (1/2)(\gamma - 1)M_\infty^2$ is the recovery temperature.

A key result of strong wall cooling $T_w \ll 1$ is that the basic flow sub-divides into two distinct zones: a main part in which $y = \mathrm{O}(1),\ \eta = \mathrm{O}(1)$ and a supplementary inner zone wherein $\eta \sim y/T_w = \mathrm{O}(T_w)$. If, for definiteness, we consider the flow at $x = 1$, then for $T_w \ll 1$ within the main part of the boundary layer we effectively have

$$U_B \approx f'(\eta), \qquad T_B \approx \left[T_r - (T_r - 1) f'\right] f',$$

where in order that both $T_B = \mathrm{O}(T_w)$ and $U_B = \mathrm{O}(T_w)$ within the inner region requires $f' \sim \widehat{d}_1 \eta$ as $\eta \to 0$ for some constant $\widehat{d}_1$. Then, in particular,

$$U_B \sim d_1 y^{1/2} + \cdots, \tag{8a}$$

$$T_B \sim e_1 y^{1/2} + \cdots, \tag{8b}$$

where $e_1 \equiv T_r d_1$ and the constant d_1 is related to $\widehat{d}_1$ by $T_r d_1^2 \equiv 2\widehat{d}_1$.

In the subregion, which we shall refer to as the buffer deck, $y = T_w^2 Y$ (or $\eta = T_w \zeta$ in terms of the Dorodnitsyn–Howarth variable). Here the basic flow is given by

$$U_B = T_w \left[\bar{u}_0 + \cdots\right], \tag{9a}$$

$$T_B = T_w \left[\overline{T}_0 + \cdots\right], \tag{9b}$$

where

$$\overline{T}_0 = \left[1 + (T_r d_1)^2 Y\right]^{1/2} = \left[1 + T_r \widehat{d}_1 \zeta\right], \tag{10a}$$

$$\bar{u}_0 = \left(\overline{T}_0 - 1\right)/T_r. \tag{10b}$$

The case of a significantly cooled wall, in which $T_w \ll T_r$ (or $S_w \ll 1$ in terms of the wall enthalpy parameter $S_w \equiv T_w/M_\infty^2$) is by no means a restricted one. It is remarked that since for large M_∞ then T_r is approximately proportional to M_∞^2, even if $T_w \ll T_r$ in high speed flow the wall temperature could still be quite appreciable. We recall that general high-speed flow $M_\infty \gg 1$ the majority of the basic boundary layer flow in the region $y = \mathrm{O}(M_\infty^2)$ has $U_B = \mathrm{O}(1)$ and $T_B = \mathrm{O}(M_\infty^2)$. The temperature adjustment layer, which is located within this $y = \mathrm{O}(M_\infty^2)$ zone, marks the point at which T_B is reduced to its O(1) values of the free-stream. For small values of S_w the inner region itself takes on a two-tiered form, with a sublayer in which $y = \mathrm{O}(M_\infty^2 S_w^2),\ U_B = \mathrm{O}(S_w),\ V_B = \mathrm{O}(M_\infty^2 S_w^3)$ and $T_B = \mathrm{O}(T_w) = \mathrm{O}(M_\infty^2 S_w)$. Thus for $M_\infty \gg 1$, $S_w \ll 1$ the wall-values for the heat transfer and skin friction have the orderings

$$\left.\frac{\partial T_B}{\partial y}\right|_{y=0} \sim S_w^{-1}, \qquad \left.\frac{\partial U_B}{\partial y}\right|_{y=0} \sim M_\infty^{-2} S_w^{-1}. \tag{11}$$

[3] For the case of a general power viscosity law this is no longer true. In a further study we have considered a more general similarity solution for the basic flow based upon a Falkner–Skan profile for which $U_B = x^m f(\widehat{\eta}),\ \widehat{\eta} = \eta x^{(m-1)/2}$ and where

$$\left[\frac{\mu_B}{T_B} f''\right]' + \frac{1}{2}(1+m) f f'' + m\left(\frac{T_B}{T_e} - (f')^2\right) = 0.$$

3. Cooled inviscid Görtler vortices

Although the properties of compressible inviscid vortices have been studied several times before, we quickly revisit this for it provides a firm footing from which we can initiate our study into the effects of cooling. The governing equations for the inviscid compressible Görtler modes are long established and here we follow Dando [27] and write

$$(u, v, w, T, p) = \big(U(y), G^{1/2}V(y), G^{1/2}W(y), T(y), GP(y)\big) \times \exp\left\{G^{1/2}\int \widetilde{\beta}(x)\,dx + i\widetilde{k}z - iG^{1/2}\int \widetilde{\Omega}(t)\,dt\right\}, \tag{12}$$

where $\widetilde{\beta}$, $\widetilde{k}$ and $\widetilde{\Omega}$ are scaled growth rates, wavenumber and frequency respectively. The substitution of (12) into (3) and the retention of the leading order terms leads to the usual compressible Görtler problem

$$\frac{d^2P}{dy^2} - \frac{2}{H}\frac{dH}{dy}\frac{dP}{dy} - \frac{\widetilde{k}^2T_B}{\widetilde{q}^2}H^2P = 0, \quad H \equiv \frac{\widetilde{q}^2}{T_B} - \frac{1}{2}\chi\frac{d}{dy}\left(\frac{U_B^2}{T_B}\right), \tag{13a}$$

or, equivalently,

$$\frac{d^2V}{dy^2} - \frac{1}{T_B}\frac{dT_B}{dy}\frac{dV}{dy} - \left[\frac{\widetilde{k}^2T_B}{\widetilde{q}^2}H^2 + \frac{T_B}{\widetilde{q}}\frac{d}{dy}\left(\frac{1}{T_B}\frac{d\widetilde{q}}{dy}\right)\right]V = 0. \tag{13b}$$

In these equations we have defined $\widetilde{q} \equiv \widetilde{\beta}U_B - i\widetilde{\Omega}$. The disturbance velocity component V and pressure P are related via $\pi_B HV = -\widetilde{q}(dP/dy)$ and are solved subject to the inviscid boundary conditions $V = 0$ or $dP/dy = 0$ at $y = 0$ and $V, P \to 0$ as $y \to \infty$.

Our concern here is confined exclusively to the case of steady modes for although the generalisation to unsteady vortices would only require a trivial modification, in the interests of brevity we do not report on this here. *Figure 2* shows the effect on the vortex growth rates of various levels of cooling on $M_\infty = 2$ boundary layer flow: we measure the degree of cooling in terms of the wall enthralpy parameter $S_w \equiv T_w/M_\infty^2$. It is observed that cooling stabilises the second and subsequent modes but has no effect at all on the first one. This is easily explained by observing that the inviscid problem (13) admits the exact eigenfunction $V = U_B(y)\exp(-\widetilde{k}y)$ with corresponding $\widetilde{\beta}^2 = \widetilde{k}\chi/2$—which is plainly independent of the degree of cooling. (We remark that Dando and Seddougui [10] noted this solution, but, unfortunately, in their version y was inadvertently replaced by the Dorodnitsyn–Howarth variable η.)

3.1. The inviscid cooled limit $T_w \to 0$

We have already shown that as $T_w \to 0$ so the basic flow in the main deck $y = \mathrm{O}(1)$ behaves as $U_B \sim d_1 y^{1/2}$, $T_B \sim e_1 y^{1/2}$ as $y \to 0$, see (8), and then analysis of (13a) demonstrates that the general solution of this equation takes the form

$$P \sim a_0\big[1 + \mathrm{O}(y)\big] + b_0\big[y^{1/2} + \mathrm{O}(y^{2/3})\big] \tag{14}$$

for $y \ll 1$. In order to solve (13a) subject to the correct boundary conditions it is necessary to establish the ratio b_0/a_0 and this is done by consideration of the buffer-deck where $y = T_w^2 Y$. Here the basic flow is as given by (9) and then (13a) leads to the result that

$$P \sim a_0 + T_w\big[a_1 + \mathrm{O}(Y^2)\big] + T_w^2\left[a_2 + \frac{\chi\widetilde{k}^2a_0}{\widetilde{\beta}^2}Y + \mathrm{O}(Y^2\ln Y) + \cdots\right] + \cdots \tag{15}$$

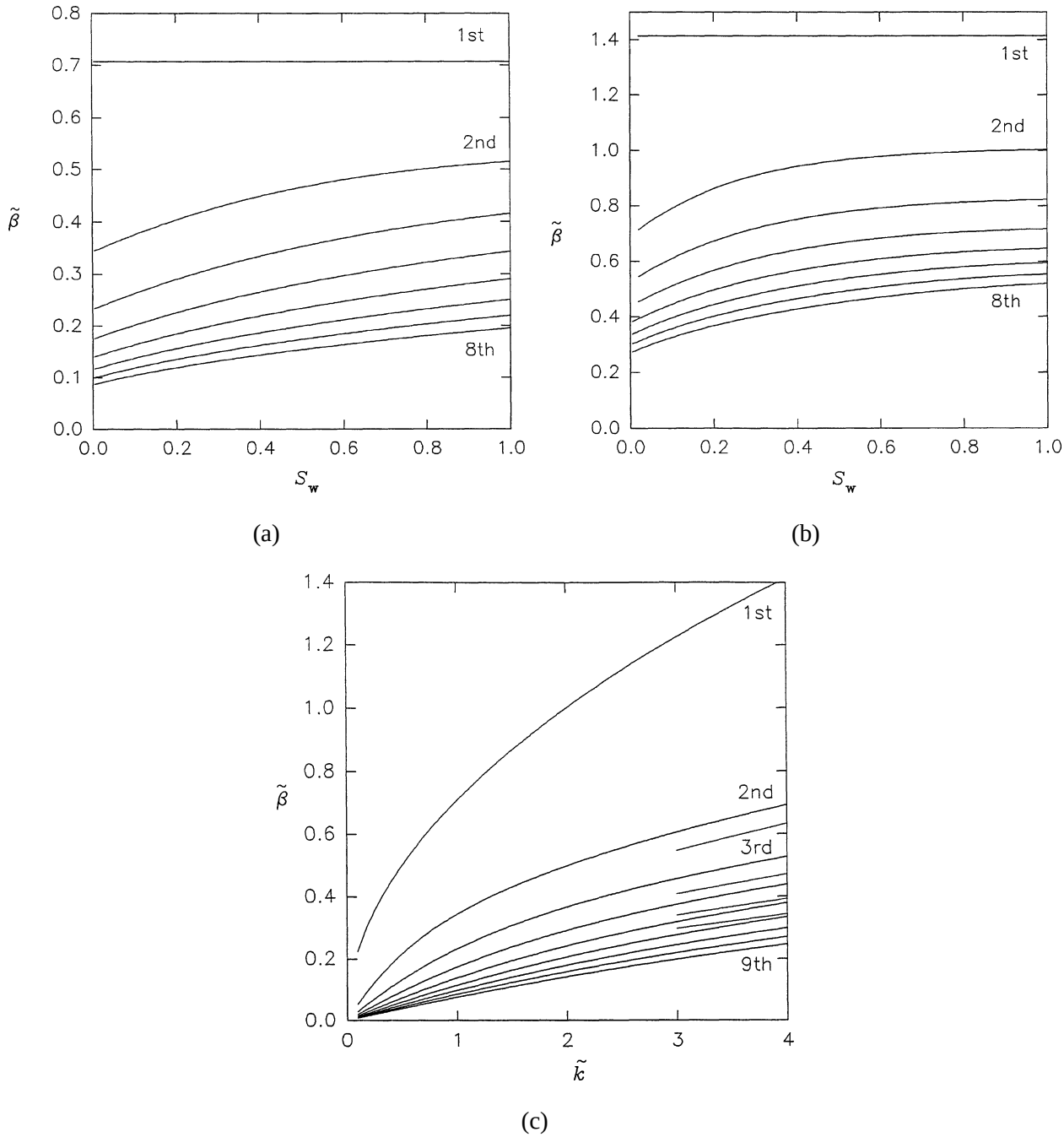

Figure 2. Effect of cooling on the growth rates $\widetilde{\beta}$ of the first eight modes in $M_\infty = 2$ flow. In (a) and (b) the wavenumber $\widetilde{k}$ is prescribed (as 1 and 4 respectively) while the degree of cooling is varied. In (c) is shown the solution of the highly cooled inviscid problem ($S_w = 0$) given by (13a) subject to $P \sim y^{1/2}$ as $y \to 0$. Here the growth rate $\widetilde{\beta}$ as a function of the wavenumber is shown with the large $\widetilde{k}$ asymptotes (17) denoted by dashed lines.

for small Y. Here a_1 and a_2 are immaterial constants and for $dP/dY = 0$ on the wall $Y = 0$ then (15) shows that $a_0 = 0$. The upshot is that for $T_w \ll 1$ the inviscid equations (13a), (13b) need to be solved subject to $P \sim \mathrm{O}(y^{1/2})$ (or $V \sim \mathrm{O}(y^{1/2})$) as $y \to 0$ rather than the perhaps more typical $dP/dy = 0$ (or $V = 0$) in this limit. The solution of this problem with slightly unfamiliar boundary conditions is shown in *figure 2(c)* which demonstrates the $\widetilde{\beta}/\widetilde{k}$ forms for the first few stationary modes. We note that this solution is very similar to those obtained with the usual inviscid inner condition for $0 < S_w \ll 1$.

3.2. The large wavenumber limit $\widetilde{k} \gg 1$

In order to access some limits of the standard inviscid configuration it is evident that the small T_w case deserves further consideration: we focus here on the wall-type modes as discussed by Dando and Seddougui [10]. When $\widetilde{k} \gg 1$ the solution structure for the wall mode in the main $y = \mathrm{O}(1)$ layer acquires a sub-layer of depth $\mathrm{O}(\widetilde{k}^{-1})$ which we shall take to lie above the $y = \mathrm{O}(T_w^2)$ buffer-deck structure adopted by the basic flow. The majority of the vortex activity is concentrated in the sub-layer where $y = \widehat{y}/\widetilde{k}$, $\widehat{y} = \mathrm{O}(1)$ and if we rescale the growth rate as $\widetilde{\beta} = \widetilde{k}^{1/2}\widehat{\beta}$ then the appropriate limit of (13b) simplifies to

$$\frac{d^2V}{d\widehat{y}^2} - \frac{1}{2\widehat{y}}\frac{dV}{d\widehat{y}} - \left[1 - \frac{\chi}{4\widehat{\beta}^2\widehat{y}} - \frac{1}{2\widehat{y}^2}\right]V = 0. \tag{16}$$

This needs to be solved subject to $V \sim \widehat{y}^{1/2}$ as $\widehat{y} \to 0$ (to match with the buffer-deck solution discussed in Section 3.1 above) and $V \sim \exp(-\widehat{y})$ as $\widehat{y} \to \infty$ for decay out of the sublayer. An analytical solution of this problem may be obtained in terms of confluent hypergeometric functions (Abramowitz and Stegun [28]) and acceptable solutions occur if

$$\widetilde{\beta}^2 = \frac{\chi\widetilde{k}}{2[1+4s]} \quad \text{for } s = 0, 1, \ldots. \tag{17}$$

This analysis for short wavelength modes holds good as long as $\widetilde{k} \ll \mathrm{O}(T_w^{-2})$. Once $\widetilde{k} = \mathrm{O}(T_w^{-2})$ the sublayer $\widehat{y} = \mathrm{O}(1)$ is no longer distinct from the buffer-deck of the basic flow. The appropriate equation for the disturbance pressure in the buffer deck becomes, in terms of the scaled Dorodnitsyn variable ζ,

$$\frac{d^2P}{d\zeta^2} - \frac{2}{H_0}\frac{dH_0}{d\zeta}\frac{dP}{d\zeta} - \frac{\widehat{k}^2\widehat{T}^2}{\widehat{q}^2}H_0^2P = 0, \tag{18}$$

where $\widetilde{k} = T_w^{-2}\widehat{k}$, $\widehat{T} = \overline{T}_0$ and $\widehat{q} = \widehat{\beta}\bar{u}_0$ (see (10)). Moreover, the scaled growth is $\widetilde{\beta} = \widehat{\beta}/T_w$ and

$$H_0^2 \equiv \widehat{q}^2 - \frac{1}{2}\chi\frac{d}{d\zeta}\left(\frac{\widehat{q}^2}{\widehat{T}}\right).$$

Equation (18) needs to be solved subject to $P \to 0$ as $\zeta \to \infty$ and $dP/d\zeta = 0$ on the wall $\zeta = 0$ and in *figure 3* we show the growth rate dependence on $\widehat{k}$ for the first eight modes. (A simple rescaling of (18) means that T_r and d_1 can be eliminated from the system and so for *figure 3* these have been set to unity.) It may be shown that for $\widehat{k} \ll 1$ the solutions of (18) match onto the wall layer modes described by (17); the mode remains effectively confined to the $\zeta = \mathrm{O}(1)$ zone while the far-field decay is brought about by through an ever thickening $\zeta = \mathrm{O}(\widehat{k}^{-1})$ region. A similar analysis, which follows that given by Dando and Seddougui [10], shows that in the opposite limit $\widehat{k} \gg 1$ the solutions of (18) match automatically to wall layer modes described

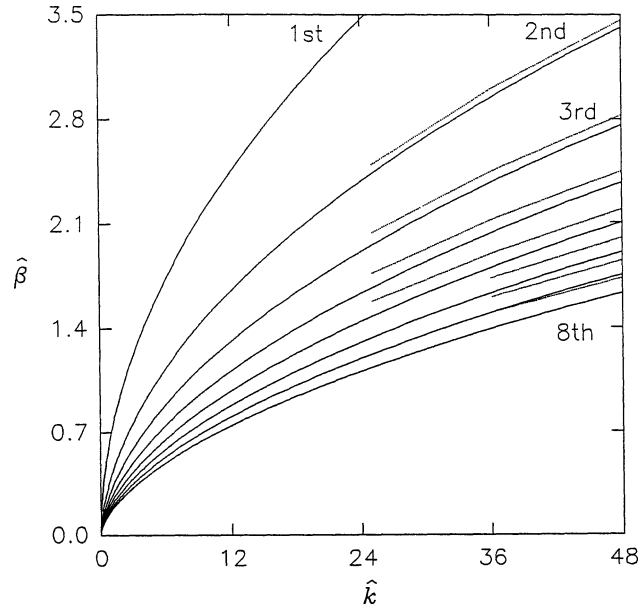

Figure 3. Solution of equation (18) for the scaled growth rate $\widehat{\beta}$ as a function of $\widehat{k}$ for the first eight modes are plotted. (The first mode is given analytically by $\widehat{\beta} = (1/2)\widehat{k}^{1/2}$.) The large $\widehat{k}$ asymptotes (19) are shown by the dashed lines.

by

$$\widehat{\beta}^2 = \frac{\chi\widehat{k}}{2[1+s]} \quad \text{for } s = 0, 1, \ldots. \tag{19}$$

Thus as $\widehat{k}$ changes from small to large values the modes evolve from one square-root behaviour to another, just as shown in *figure 3*. Lastly, we note that the limit $\widehat{k} \to \infty$ indicates that for sufficiently large $\widehat{k}$ the effect of cooling on inviscid modes is ultimately to push the fastest growing vortex to ever decreasing wavelengths.

The analysis summarised above suggests that the scaling $\widetilde{\beta} \sim \widetilde{k}^{1/2} T_w^{-1}$ must mark a significant dividing line because as for smaller values of $\widetilde{k}$ the region of vortex activity lies outside the buffer deck so the problem is essentially inviscid. However, as the wall temperature $T_w \to 0$ the vortex increasingly concentrates itself inside the buffer and a new viscous interaction problem must come into play. We shall describe this situation as arising in the case of severe wall cooling and return to explore its properties in Section 6. Meantime, we conduct an analysis parallel to that already undertaken with the object of addressing the question as to the fate of long wavelength interactive Görtler vortices as the wall is gradually cooled.

4. The moderately cooled interactive structure

Timoshin [7] was the first to note the connection between triple-deck theory (see Smith [29] for an excellent review) and Görtler vortices. Somewhat later, Choudhari et al. [14] showed that Görtler vortices within an incompressible boundary layer are governed by the interactive viscous-inviscid mechanism of Rozhko and Ruban [13] once the spanwise wavenumber drops to $O(G^{-1/7})$ (region IV on *figure 1*). The relevant structure consists of zones of depths $O(G^{-1/7})$, $O(1)$ and $O(G^{1/7})$ relative to the boundary layer thickness and CHS [14] derived the linearised dispersion relations for the vortices. This eigenrelation represents a balance between the

effects of viscosity in the lower deck, of destabilising centrifugal forces in the main deck and of viscous–inviscid interaction in the uppermost region.

A repetition of the arguments discussed by Rozhko and Ruban [13], generalised to include the effects of both wall cooling and large Mach numbers, show that unsteady vortices are described by a triple-deck like configuration in the vicinity of (x_0, z_0) with streamwise, spanwise and time scales given by

$$(x - x_0, z - z_0, t) \sim \left(G^{-3/7} S_w^{6/7} M_\infty^{12/7}, G^{1/7} S_w^{12/7} M_\infty^{24/7}, G^{-2/7} S_w^{4/7} M_\infty^{8/7}\right). \tag{20}$$

Here we are assuming that S_w is O(1) or small and M_∞ is O(1) or large. For $S_w \ll 1$ it has already been shown in Section 2 how the main part of the basic boundary layer sub-divides and develops a buffer region lying above the viscous wall layer. Based upon the scalings implicit within (20), it is a routine task to show that while the upper and lower decks in the interactive structure are of thicknesses $y \sim G^{1/7} S_w^{12/7} M_\infty^{24/7}$ and $y \sim G^{-1/7} S_w^{9/7} M_\infty^{18/7}$ respectively, the main deck for which $y \sim M_\infty^2$ acquires a buffer zone where $y \sim M_\infty^2 S_w^2$.

A number of new limits may arise as S_w and/or M_∞ vary from O(1) values. One way in which the interactive structure breaks down occurs should the upper and main decks coincide. This happens if

$$S_w \sim M_\infty^{-5/6} G^{-1/12}. \tag{21a}$$

Non-parallel effects can also affect our analysis and do so should the lengthscale of the vortex grow so as to be comparable with the distance over which the basic flow develops and this occurs once

$$S_w \sim M_\infty^{-2} G^{1/2}. \tag{21b}$$

In particular, in the adiabatic case for which $S_w = \mathrm{O}(1)$, nonparallelism is significant once $M_\infty \sim G^{1/4}$. Another mechanism through which the interactive structure may fail is concerned with the transition layer that divides the main deck and freestream when both $M_\infty \gg 1$ and $S_w \ll 1$. It is well known that on a flat plate the transition zone marks the rapid change between the relatively high $\mathrm{O}(M_\infty^2)$ basic temperature of the main deck and the much cooler O(1) freestream flow. Analysis of the vertical velocity component of the disturbance within the transition region shows that its form becomes disordered and therefore has to be modified once

$$S_w \sim M_\infty^{1/3} G^{-1/12}. \tag{21c}$$

Finally, it is noted in passing that the buffer and lower decks of the structure merge when

$$S_w \sim M_\infty^{4/5} G^{-1/5}. \tag{21d}$$

Relationships (21a)–(21d) are sketched in *figure 4*. It is noted how that as M_∞ and/or S_w are varied from O(1) values so it is possible that modifications to our interactive structure might be required due to any of (21a)–(21c) being achieved. Naturally, which of these is relevant depends on the location in S_w/M_∞ parameter space.

Since the focus in this work has been to ascertain how wall cooling can affect Görtler vortices, without the additional complication of non-parallelism, *figure 4* suggests that most interest would be in the case of limit (21a) when the upper and main decks coincide. For definiteness, and to contrast with previous, mainly hypersonic investigations, we fix $M_\infty = \mathrm{O}(1)$ which implies $T_w = \mathrm{O}(G^{-1/12})$.[4] In the ensuing analysis it is

[4] We have also applied the scalings to consider the effect of nonlinearity on this structure. This enters the problem via the viscous sublayer where the unsteady boundary-layer equations govern the flow.

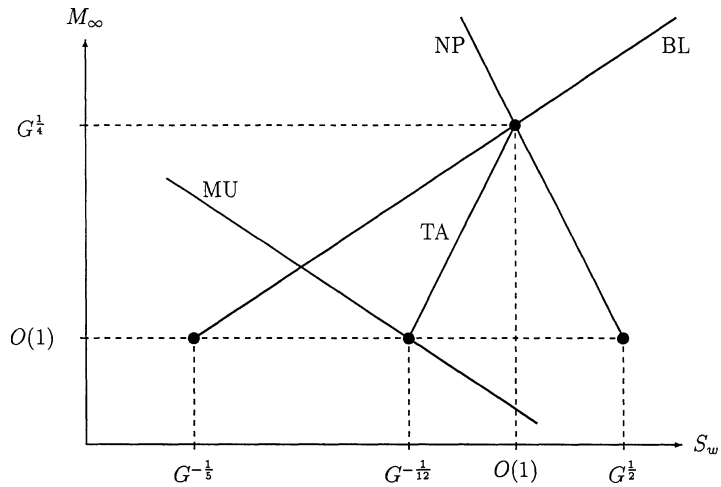

Figure 4. The regions in M_∞/S_w parameter space which mark the limits of validity of the cooled interactive structure of CHS. The lines indicate when the middle and upper decks merge (MU); when nonparallel effects become important (NP); when the solution in the temperature adjustment region requires modification (TA) and when the buffer and lower decks coincide (BL).

convenient to define the small parameter

$$\widetilde{\varepsilon} = G^{-1/12}. \tag{22}$$

Then, in order to examine vortices at $x = x_0$, appropriate new variables are

$$x = x_0 + \widetilde{\varepsilon}^6 \widetilde{X}, \qquad t = \widetilde{\varepsilon}^4 \widetilde{t} \tag{23}$$

and the wall temperature $T_w = \mathrm{O}(\widetilde{\varepsilon})$. The arguments rehearsed above show that the perturbation structure is composed of a main region in which $y = \mathrm{O}(1)$, a buffer zone with $y = \mathrm{O}(\widetilde{\varepsilon}^2)$ and the wall layer where $y = \mathrm{O}(\widetilde{\varepsilon}^3)$.

4.1. The buffer region: $y = \widetilde{\varepsilon}^2 \widetilde{y}$

Solutions of the linearised disturbance equations are sought of the form

$$(u, v, w, P, \rho, T) = \left(\widetilde{u}_1, \widetilde{\varepsilon}^{-4}\widetilde{v}_1, \widetilde{\varepsilon}^{-5}\widetilde{w}_1, \widetilde{\varepsilon}^{-11}\widetilde{p}_1, \widetilde{\varepsilon}^{-2}\widetilde{\rho}_1, \widetilde{T}_1\right) E + \text{c.c.}, \tag{24}$$

where $E \equiv \exp[\beta \widetilde{X} + i(kz - \Omega \widetilde{t})]$, c.c. denotes complex conjugate and the unknowns are functions of $\widetilde{y}$. At leading order the basic flow is given by

$$\overline{T}_0 = \left[\widetilde{T}_w^2 + 2\bar{s}\widetilde{y}\right]^{1/2}, \tag{25a}$$

$$\bar{u}_0 = \frac{\bar{\lambda}}{\bar{s}}\left[\overline{T}_0 - \widetilde{T}_w\right], \tag{25b}$$

with the wall temperature $T_w = \widetilde{\varepsilon}\,\widetilde{T}_w$ and the constants $\bar{\lambda}$ and $\bar{s}$ are related to the main-deck values d_1 and e_1 (8) by $e_1 = \sqrt{2\bar{s}}$, $d_1\bar{s} = e_1\bar{\lambda}$. On substituting (23) and (24) into (3) we find that the leading order disturbance solutions in the buffer zone are given by

$$\widetilde{u}_1 = A_1 \frac{d\bar{u}_0}{d\widetilde{y}}, \tag{26a}$$

$$\widetilde{v}_1 = -\beta A_1 \bar{u}_0, \tag{26b}$$

$$\widetilde{\rho}_1 = A_1 \frac{d\bar{\rho}_0}{d\widetilde{y}}, \tag{26c}$$

$$\widetilde{T}_1 = A_1 \frac{d\bar{T}_0}{d\widetilde{y}}, \tag{26d}$$

$$\widetilde{p}_1 = P_1, \tag{26e}$$

$$\widetilde{w}_1 = \frac{ikP_1}{\beta\bar{\rho}_0\bar{u}_0}, \tag{26f}$$

where A_1 and P_1 are unknown displacement and pressure constants respectively.

4.2. The wall layer: $y = \widetilde{\varepsilon}^{\,3}\widetilde{Y}$

Here we find it convenient to scale the disturbance on $\bar{\lambda}_1$, $\widetilde{R}_w$, $\widetilde{T}_w$ and $\widetilde{\mu}_w$ which denote the (scaled) wall-values of the basic shear, density, temperature and viscosity respectively. In this wall layer the disturbance takes the form

$$(u, v, w, P, \rho, T, \mu) = \left(\bar{\lambda}_1 b\,\widetilde{U},\ \widetilde{\varepsilon}^{-3}\bar{\lambda}_1 b^2\,\widetilde{V},\ \widetilde{\varepsilon}^{-6}\bar{\lambda}_1 b\,\widetilde{W},\ \widetilde{\varepsilon}^{-11}\widetilde{R}_w\bar{\lambda}_1^2 b^2\,\widetilde{P},\ \widetilde{\varepsilon}^{-2}\widetilde{\rho},\ \widetilde{T},\ \widetilde{\mu}\right)E + \text{c.c.},$$

where $b^3 \equiv \widetilde{T}_w^3\widetilde{C}(\bar{\lambda}_1\pi_B)^{-1}$ and by assumption $\widetilde{\mu}_w = \widetilde{C}\widetilde{T}_w$ and $\widetilde{R}_w\widetilde{T}_w = \pi_B$. On rescaling

$$\left(A_1, \widetilde{Y}, \widetilde{t}\,\right) \to \left(b\widetilde{A}, b\widetilde{Y}, \widetilde{t}/b\bar{\lambda}_1\right)$$

we obtain at a standard viscous layer problem whose solution leads to the pressure–displacement relationship

$$\frac{\widetilde{P}}{\widetilde{A}} = -\frac{\beta^{5/3}}{k^2}\frac{\mathrm{Ai}'(\xi_0)}{\left(\int_{\xi_0}^{\infty}\mathrm{Ai}(s)\,ds\right)}, \quad \xi_0 \equiv -\frac{i\Omega}{\beta^{2/3}}.$$

4.3. The main tier: $y = \mathrm{O}(1)$

Last comes the uppermost region in the disturbance structure. The buffer zone solutions of Section 4.1 suggest that here the leading order disturbance solutions acquire the forms

$$(u, v, w, P, \rho, T) = \left(\widetilde{\varepsilon}\,\widetilde{u},\ \widetilde{\varepsilon}^{-5}\widetilde{v},\ \widetilde{\varepsilon}^{-5}\widetilde{w},\ \widetilde{\varepsilon}^{-11}\widetilde{p},\ \widetilde{\varepsilon}\,\widetilde{\rho},\ \widetilde{\varepsilon}\,\widetilde{T}\right)E + \text{c.c.}, \tag{27}$$

and the consequent perturbation equations can be reduced to a coupled pair for $\widetilde{v}$ and the pressure $\widetilde{p}$ which together satisfy

$$\beta\frac{\pi_B}{T_B}\left[U_B\frac{\partial\widetilde{v}}{\partial y} - \frac{\partial U_B}{\partial y}\widetilde{v}\right] = -k^2\widetilde{p}, \tag{28a}$$

$$\beta U_B\frac{\partial\widetilde{p}}{\partial y} = \frac{\pi_B}{T_B^2}\left[-\beta^2U_B^2 + \frac{1}{2}\chi T_B\frac{\partial}{\partial y}\left(\frac{U_B^2}{T_B^2}\right)\right]\widetilde{v}. \tag{28b}$$

This system needs to be solved subject to appropriate decay conditions as $y \to \infty$ and matching to the buffer solutions as $y \to 0$. It is convenient to non-dimensionalise $\widetilde{v}$ and $\widetilde{p}$ using

$$(\widetilde{v}, \widetilde{p}) \to \left(d_1 b\widetilde{v}, \widetilde{R}_w\bar{\lambda}_1^2 b^2\widetilde{p}\right),$$

where the constant d_1 arises from the solution of the basic flow in the buffer deck, see (8). It is also useful to define a scaled surface temperature

$$\widetilde{\tau} \equiv \sqrt{2}\left(\frac{\pi_B}{\widetilde{C}}\right)^{1/3} \widetilde{s}_1^{\,-3/2} \widetilde{T}_w^2, \tag{29}$$

with $(\partial T_B/\partial y)|_{y=0} = \widetilde{s}_1/T_w$. (Note that this definition of $\widetilde{\tau}$ is a direct counterpart of the cooling parameter τ introduced in the work of Seddougui et al. [19].) With these simplifications we can reduce (28) to a single equation for $\widetilde{p}$ which, with $\bar{\widetilde{q}} \equiv \beta U_B$, may be cast as

$$\frac{\partial^2 \widetilde{p}}{\partial y^2} - \frac{2}{H}\frac{dH}{dy}\frac{\partial \widetilde{p}}{\partial y} - k^2\left\{1 - \frac{1}{2}\chi \frac{T_B}{\bar{\widetilde{q}}^2}\frac{\partial}{\partial y}\left(\frac{U_B^2}{T_B}\right)\right\}\widetilde{p} = 0, \tag{30}$$

in which

$$H^2 \equiv \frac{\bar{\widetilde{q}}^2}{T_B} - \frac{1}{2}\chi \frac{\partial}{\partial y}\left(\frac{U_B^2}{T_B}\right).$$

This equation is actually almost identical to system (13) with the only modification resulting from the changed near-wall behaviour of the basic flow as in Section 2. It is also a long-wavelength version of the governing equation for moderately cooled Tollmien–Schlichting waves in compressible flow but supplemented by terms which account for the presence of curvature. In order to match with the buffer deck solutions we need to solve (30) subject to

$$\widetilde{p} \sim \widetilde{P}\left[1 + \mathrm{O}(y) + \cdots\right] - \frac{1}{2}\widetilde{\tau}\chi\widetilde{A}\left[y^{1/2} + \cdots\right] \quad \text{as } y \to 0; \tag{31}$$

in addition the far-field decay $\widetilde{p} \to 0$ needs to be imposed and the pressure–displacement law (27) satisfied.

It is the small-y behaviour (31) which distinguishes this problem from many similar ones. Typically (see Section 3.1) the physically relevant solution of equations akin to (30) is the one that diminishes as rapidly as possible for small y so that, in the current context, this requires setting $\widetilde{P} = 0$. Here, however, the combination of the buffer deck solutions together with the pressure–displacement law (27) fixes the relationship (31) so that both small-y forms are components of the required solution.

5. Solution of the interactive problem

Here we describe solutions of the linearised equations governing our moderately cooled modes and do so with the curvature parameter in (30) set to be unity. The numerical method required a careful coupling of (27) and (31) and was based on a scheme developed by Elliott and Strange [30] for investigating moderately cooled Tollmien–Schlichting waves. Unlike the method employed by Seddougui et al. [19], who used a test function for the basic flow quantities, our technique used the Dorodnitsyn variable and the similarity solutions discussed in Section 2.1. (We remark that the approach was also capable of accounting for both a general power viscosity law and Falkner–Skan similarity forms.) Equation (30) was solved subject to decay for large y which furnishes an estimate for the ratio $\widetilde{P}/\widetilde{A}$ obtained from the small y behaviour (31). In general this ratio does not fulfill the pressure–displacement relation (27) with Ω real so iteration on the spatial development parameter β was performed so as to ensure that this constraint was satisfied.

Our first results are concerned with stationary modes as the scaled cooling parameter $\widetilde{\tau}$ (see (29)) is varied. *Figure 5* shows the dependence of the spatial growth rate $\mathrm{Re}(\beta) \equiv \beta_r$ of the first eight modes at wavenumbers

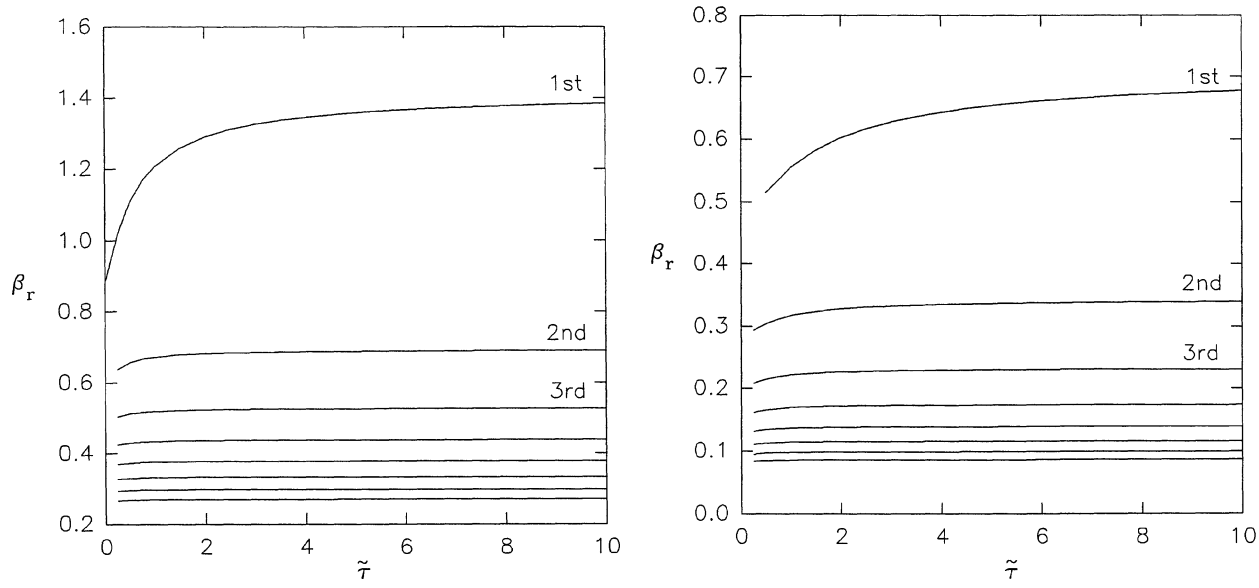

Figure 5. Growth rates β_r as functions of cooling parameter $\tilde{\tau}$ for the first eight interactive moderately cooled modes of (27), (30) and (31). (a) Wavenumber $k = 1$, (b) $k = 4$.

$k = 1$ and $k = 4$. A noteworthy feature of these results is that the growth rates are quite insensitive to the degree of cooling applied and it is only the first mode that shows much dependence on $\tilde{\tau}$ as $\tilde{\tau} \to 0$. These modes are the natural extensions of those steady disturbances studied by Dando and Seddougui [10] taken into the moderately cooled regime. However our computations also revealed the existence of another family of unsteady solutions which appear to be disconnected from the previously known ones. Properties of neutrally stable manifestations of our novel modes are shown in *figure 6* which illustrates the values of the streamwise wavenumber α_n ($\equiv \mathrm{Im}(\beta)$) and neutral frequency Ω_n as functions of k for a selection of cooling parameters $\tilde{\tau}$. Two branches of solutions exist: for prescribed $\tilde{\tau}$ then as the spanwise wavenumber $k \to 0$ so on one branch $\alpha_n \to 0$ while on the other $\alpha_n \to \infty$. An almost identical plot is obtained of these neutral characteristics if we interchange the roles of k and $\tilde{\tau}$. *Figure 7* shows the neutral properties as functions of $\tilde{\tau}$ with k/α^2 held fixed. We see that as $\tilde{\tau} \to \infty$ both α_n and $\Omega_n \to 0$ and presumably this limit matches to the uncooled non-stationary neutral modes of the CHS [14] regime. Conversely, as $\tilde{\tau} \to 0$ both α_n and $\Omega_n \to \infty$ and link onto the severely cooled regime that we will discuss later.

Figure 8 is focussed on the question of the spatial development properties of our new modes. Here we have plotted the growth rate β_r and the streamwise wavenumber β_i as functions of Ω for various degrees of cooling. These results relate to the spanwise wavenumber $k = 1$ and one feature of particular note is the existence of a cut-off for $\Omega \ll 1$; if we denote this cut-off as Ω_c then no solutions exist for $\Omega < \Omega_c$. It was found numerically that as $\Omega \to \Omega_c$ then $\beta \to 0$ such that $\xi_0 = -i^{1/3}\Omega/\beta^{2/3} \to \infty$. (Our calculations suggested that the cut-off occurs at $\Omega_c \approx 0.55\tilde{\tau}$.) In the opposite limit $\Omega \to \infty$ so ξ_0 tends to a constant value and it is remarked that the growth rate β_r increases without bound. One last interpretation of the new modes is presented in *figure 9* which is concerned with the behaviours of disturbances with $\Omega/\tilde{\tau}$ fixed. The results are suggestive of the appearance of a high-frequency upper branch structure similar to that for Tollmien–Schlichting waves—a result which can also be obtained by a high frequency analysis of the dispersion relation. We note that for $\Omega/\tilde{\tau}$ fixed, then as $\tilde{\tau}$ increases we have a maximum growth rate at some finite value of $\tilde{\tau}$ before the growth rate tends to zero.

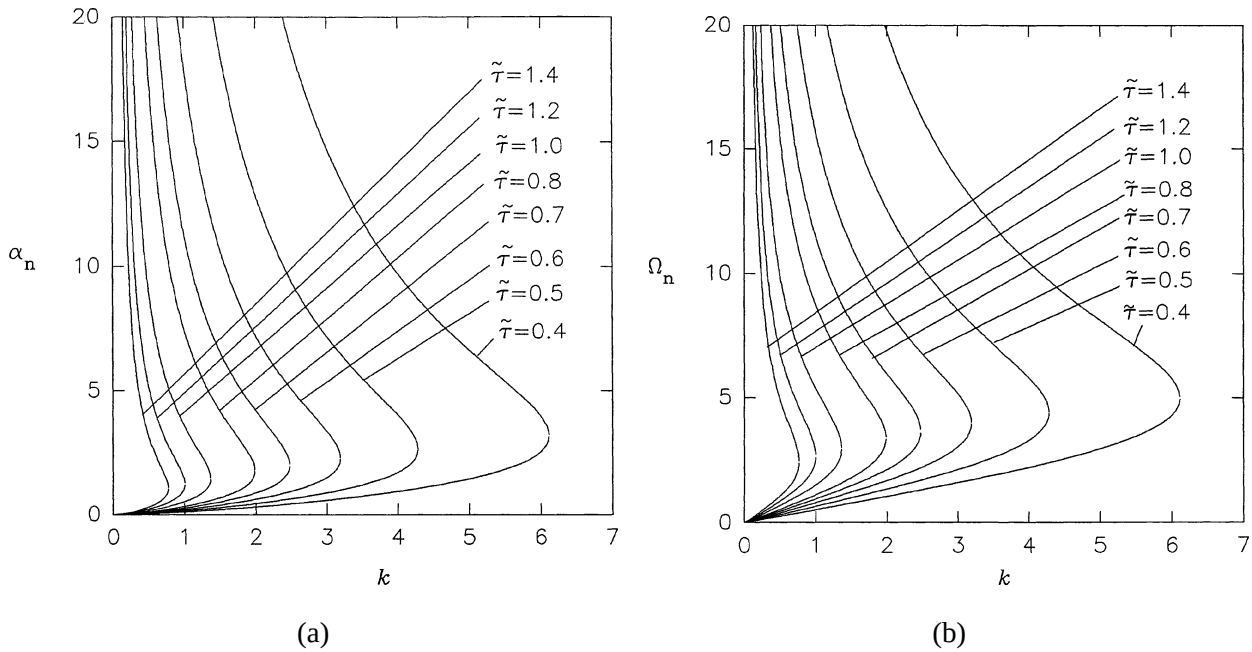

Figure 6. Neutral modes as functions of spanwise wavenumber k for prescribed wall cooling $\widetilde{\tau}$. (a) Streamwise wavenumber α_n and (b) frequency Ω_n. The parameter space to the right of the curves delimits the unstable region.

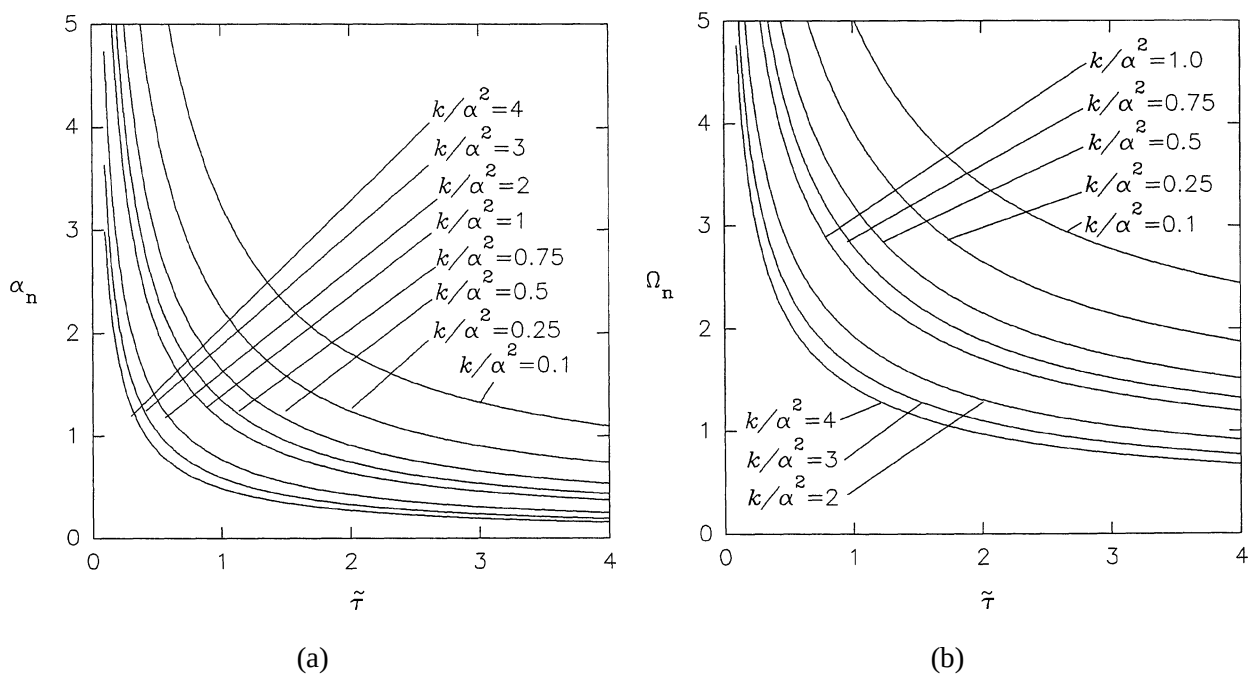

Figure 7. Neutral modes as functions of $\widetilde{\tau}$ for prescribed values of k/α^2. (a) Streamwise wavenumber α_n and (b) frequency Ω_n.

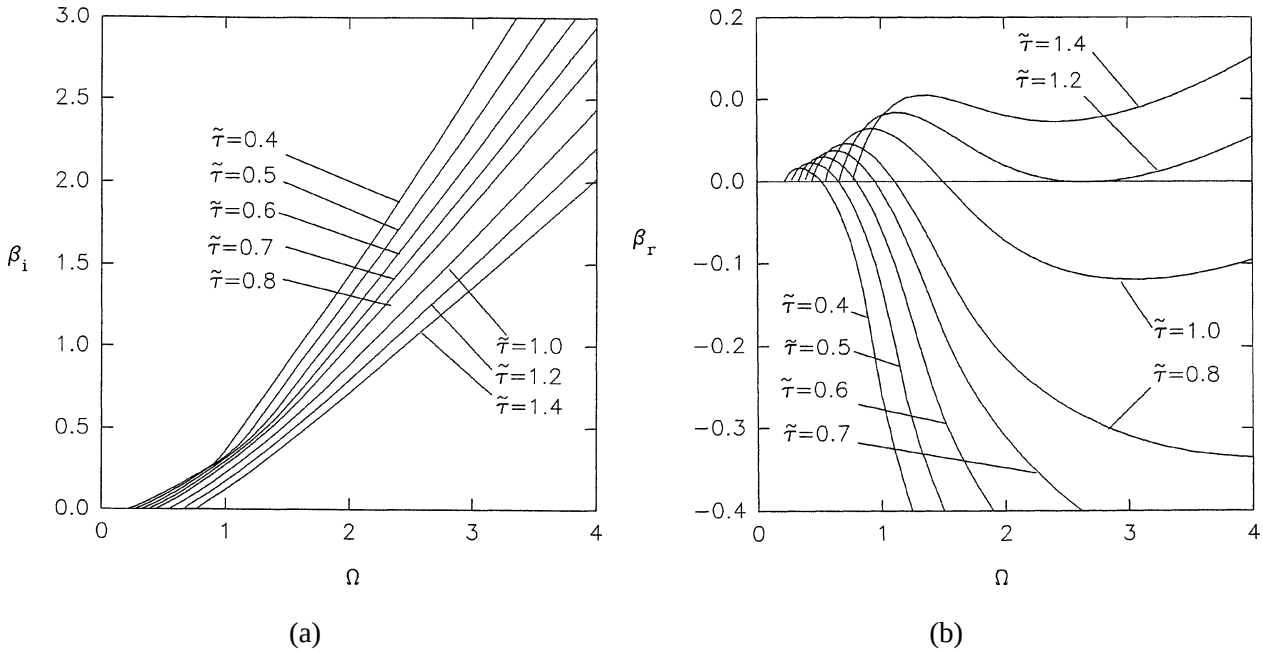

Figure 8. Non-neutral interactive modes of wavenumber $k = 1$ as functions of vortex frequency Ω for various values of wall cooling $0.4 \leqslant \tilde{\tau} \leqslant 1.4$. (a) Streamwise wavenumber β_i and (b) spatial growth rate β_r. Note that in (b) all the curves turn and $\beta_r \to \infty$ as $\Omega \to \infty$.

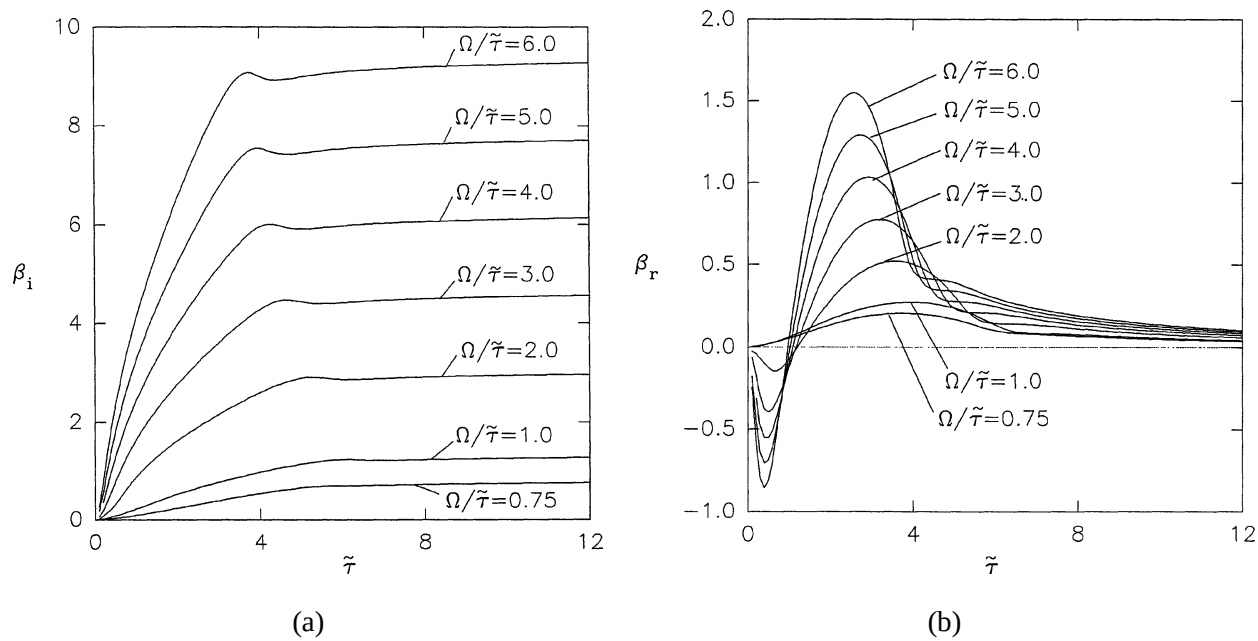

Figure 9. Non-neutral modes of wavenumber $k = 1$. (a) Streamwise wavenumber β_i and (b) spatial growth rate β_r as functions of wall cooling $\tilde{\tau}$ for prescribed frequency/cooling ratios $0.75 \leqslant \Omega/\tilde{\tau} \leqslant 6$.

A few important points should be made about these findings. It appears that for each fixed $\tilde{\tau}$ there is a maximum spatial vortex growth rate: these maximums diminish as $\tilde{\tau} \to \infty$ and for fixed $\Omega/\tilde{\tau}$ and $\tilde{\tau} \gg 1$ we appear to have a match to upper-branch-like inviscid problems. Of course, there are a number of features of this moderately cooled structure that could be taken further and we hope to examine some of the aspects in further studies, but we do not attempt to discuss more limits here. Instead we now switch our attention back to the new severely cooled vortex disturbances that we predicted as a result of our analysis in Section 3.

6. The severely cooled mode

Let us recall the information portrayed in *figure 1* and make particular note of the modes I–III; that is the right-hand branch, the regime containing the most amplified mode (at least in the case of zero crossflow) and the inviscid vortices respectively. We have already shown, in Section 3, that the effect of a gradual cooling from the adiabatic state of the inviscid modes of Dando and Seddougui [10] is the introduction of some new viscous interaction that comes into play as the wall temperature $T_w \to 0$. In Section 4 we obtained one new form, the moderately cooled mode. Now we pursue a second, more dangerous form, and begin by noting a somewhat surprising connection between these modes and the I–III structures that arise in adiabatic flow.

It is convenient, as in Section 4, to account for the effect of large M_∞ as well as wall cooling by taking $S_w = T_w/M_\infty^2 \ll 1$ and assuming that M_∞ is either O(1) or large. Let us now consider the parameter regimes for cooling at which each of the mode types I–III are first significantly affected. Notice that for each of the three modes discussed below the relevant scales for density and temperature are given by

$$(\rho, T) \sim \left(M_\infty^{-2} S_w^{-2} u, M_\infty^2 u\right),$$

where the size of u is arbitrary.

6.1. The parameter regimes

6.1.1. The right-hand branch

We recall that the right-hand branch mode I for incompressible flow was first studied by Hall [4] and was subsequently extended to compressible flows by Hall and Malik [9]. The vortex activity is concentrated in a thin region within the cooled sublayer and the relevant scales are

$$(x, y, z, t) \sim \left(G^{-1/2} M_\infty S_w, G^{-1/8} M_\infty^{9/4} S_w^{3/2}, G^{-1/4} M_\infty^{5/2} S_w, G^{-3/8} M_\infty^{3/4} S_w^{1/2}\right), \tag{32a}$$

$$(v, w, P) \sim \left(G^{1/2} M_\infty S_w u, G^{3/8} M_\infty^{5/4} S_w^{1/2} u, G^{5/8} M_\infty^{3/4} S_w^{1/2} u\right). \tag{32b}$$

6.1.2. The most amplified mode

The mode II vortex structure is concentrated in a region below the cooled sublayer of the basic flow and is associated with the scales

$$(x, y, z, t) \sim \left(G^{-3/5} M_\infty^{6/5} S_w^{3/5}, G^{-1/5} M_\infty^{12/5} S_w^{6/5}, G^{-1/5} M_\infty^{12/5} S_w^{6/5}, G^{-2/5} M_\infty^{4/5} S_w^{2/5}\right), \tag{33a}$$

$$(v, w, P) \sim \left(G^{2/5} M_\infty^{6/5} S_w^{3/5} u, G^{2/5} M_\infty^{6/5} S_w^{3/5} u, G^{3/5} M_\infty^{4/5} S_w^{2/5} u\right). \tag{33b}$$

6.1.3. The inviscid modes

Based on the assumption that vortex activity for inviscid modes takes place within the cooled sublayer, an analysis of stability equations (3) shows that the relevant length and time scales are

$$(x, y, z, t) \sim \left(G^{-1/2}M_\infty S_w, M_\infty^2 S_w^2, M_\infty^2 S_w^2, G^{-1/2}M_\infty\right), \tag{34a}$$

$$(v, w, P) \sim \left(G^{1/2}M_\infty S_w u, G^{1/2}M_\infty S_w u, G S_w^2 u\right). \tag{34b}$$

It is seen that for the case $S_w \sim G^{-1/4}M_\infty^{1/2}$ all three of the above modes collapse into the same single structure. Since $S_w \ll 1$ for a highly-cooled sublayer and $x^{-1} \gg 1$ to avoid nonparallelism we conclude that the regime of interest is

$$\mathrm{O}(1) \leqslant M_\infty \ll G^{1/2}, \qquad G^{-1/4} \ll S_w \ll 1. \tag{35}$$

6.2. The severely cooled limit

For definiteness, and to contrast with the work of Bogolepov [26], we shall fix $M_\infty = \mathrm{O}(1)$ which suggests the wall temperature scaling

$$T_w = G^{-1/4}\widehat{T}_w, \tag{36}$$

with $\widehat{T}_w$ assumed to be an O(1) parameter. This choice also provides a link with the cooled inviscid modes of Section 3.1 where $\beta = G^{1/2}\widetilde{\beta} \sim G^{1/2}\widetilde{k}^{1/2} \sim G^{1/2}T_w^{-1}$. For if in that formulation we reduce $T_w = \mathrm{O}(G^{-1/4})$ then $\widetilde{k} \sim G^{1/2}$, $\widetilde{\beta} \sim G^{1/4}$ and then the overall wavenumber of the modes becomes $\beta \sim G^{3/4}$. (There is also a connection between these modes and the moderately cooled forms of Section 5, which will be discussed later.)

These severely cooled modes evolve over an $\mathrm{O}(G^{-3/4})$ lengthscale so it is convenient to define

$$x - x_0 = G^{-3/4}X, \qquad y = G^{-1/2}Y, \qquad z - z_0 = G^{-1/2}Z, \qquad t = G^{-1/2}\widehat{t}, \tag{37a}$$

and write the basic flow

$$(U_B, V_B, R_B, T_B, \mu_B, P_B) = \left(G^{-1/4}\overline{U}, G^{-3/4}\overline{V}, G^{1/4}\overline{R}, G^{-1/4}\overline{T}, G^{-1/4}\bar{m}, G^{-1/4}\overline{P}\right), \tag{37b}$$

together with the disturbance

$$(u, v, w, P, \rho, T) = \left(\widehat{u}, G^{1/4}\widehat{v}, G^{1/4}\widehat{w}, G^{1/2}\widehat{P}, G^{-1/2}\widehat{\rho}, \widehat{T}\right)E + \text{c.c.}, \tag{37c}$$

where $E \equiv \exp(\beta X + ikZ - i\Omega\widehat{t})$. These scalings are introduced into system (3) and after some manipulation it turns out that it is convenient to define the quantities

$$\bar{q} = \beta\overline{U} - i\Omega, \tag{38a}$$

$$\widehat{Q} = \frac{d}{dY}\left[\frac{d\widehat{v}}{dY} - \frac{1}{\overline{T}}\left(\bar{q}\widehat{T} + \frac{d\overline{T}}{dY}\widehat{v}\right)\right] - k^2\widehat{v}. \tag{38b}$$

For $Y = \mathrm{O}(1)$ we have

$$\overline{T} = \left[\widehat{T}_w^2 + 2\bar{s}Y\right]^{1/2}, \tag{39a}$$

$$\overline{U} = \frac{\bar{\lambda}}{\bar{s}}\left\{\left[\widehat{T}_w^2 + 2\bar{s}Y\right]^{1/2} - \widehat{T}_w\right\}, \tag{39b}$$

$$\overline{P} = \overline{P}_0 - \frac{\bar{\lambda}\chi}{2\bar{s}^2}\pi_B\left\{\frac{1}{3}\left[\widehat{T}_w^2 + 2\bar{s}Y\right]^{3/2} - 2\bar{s}Y + \left[\widehat{T}_w^2 + 2\bar{s}Y\right]^{1/2}\right\}, \tag{39c}$$

where the constants $\bar{\lambda}$ and $\bar{s}$ are scaled values of the heat transfer and the skin friction of the basic boundary layer. In order to scale out as many parameters as possible we define

$$Y = b^{-1}Y_D, \qquad \beta = a\beta_D, \qquad \Omega = \frac{a\bar{\lambda}}{\sqrt{b\bar{s}}}\Omega_D, \qquad \widehat{T}_w = \left(\frac{b}{\bar{s}}\right)^{1/2} T_{Dw} \tag{40}$$

and

$$(\overline{U}, \overline{T}, \bar{m}, \bar{q}) = \left[\frac{\bar{\lambda}}{\sqrt{b\bar{s}}}\bar{U}_D, \left(\frac{\bar{s}}{b}\right)^{1/2}\bar{\theta}_D, C\left(\frac{\bar{s}}{b}\right)^{1/2}\bar{m}_D, \frac{a\bar{\lambda}}{\sqrt{b\bar{s}}}\bar{q}_D\right], \tag{41a}$$

$$(\widehat{u}, \widehat{v}, \widehat{w}, \widehat{T}, \widehat{Q}) = \left[\widehat{u}_D, \frac{a}{b}\widehat{v}_D, \frac{a}{b}\widehat{w}_D, \frac{\bar{s}}{\bar{\lambda}}\widehat{T}_D, ab\widehat{Q}_D\right], \tag{41b}$$

where the constants a and b are to be fixed. Furthermore,

$$\bar{\theta}_D = \left[T_{Dw}^2 + 2Y_D\right]^{1/2}, \qquad \overline{U}_D = \bar{\theta}_D - T_{Dw}, \qquad \bar{m}_D = \bar{\theta}_D, \qquad \bar{q}_D = \beta_D\overline{U}_D - i\Omega_D, \tag{42}$$

and then we define

$$\Pi = \frac{\pi_B\bar{\lambda}|\chi|^{1/2}}{C}\bar{s}^{-3/2} \quad \Rightarrow \quad a = |\chi|^{1/2}\Pi^{1/2}, \quad b = \Pi. \tag{43}$$

The solutions presented below are all given in terms of the dimensionless variables with a subscript D but it was found that the numerical side of the solution process could be simplified in the following way. Another parameter can be removed from the problem by scaling the flow variables on the vortex wavenumber k and writing

$$Y_D = \frac{1}{k}\widehat{Y}, \qquad \beta_D = \varepsilon\widehat{\beta}, \qquad \Omega_D = \frac{\varepsilon}{\sqrt{k}}\widehat{\Omega}, \qquad \tau = \sqrt{k}T_{Dw}, \tag{44a}$$

and also

$$(\overline{U}_D, \bar{\theta}_D, \bar{q}_D) = \left[\frac{1}{\sqrt{k}}\bar{u}, \frac{1}{\sqrt{k}}\bar{\theta}, \frac{\varepsilon}{\sqrt{k}}\bar{q}\right]. \tag{44b}$$

The transformed basic flow is then given by

$$\bar{\theta} = \left[\tau^2 + 2\widehat{Y}\right]^{1/2}, \qquad \bar{u} = \bar{\theta} - \tau, \qquad \bar{q} = \widehat{\beta}\bar{u} - i\widehat{\Omega}, \tag{45}$$

and if the perturbation quantities are scaled with

$$(\widehat{u}_D, \widehat{v}_D, \widehat{w}_D, \widehat{T}_D, \widehat{Q}_D) = \left[\widehat{\widehat{u}}, \frac{\varepsilon}{k}\widehat{\widehat{v}}, \frac{\varepsilon}{k}\widehat{\widehat{w}}, \widehat{\widehat{T}}, \varepsilon k\widehat{\widehat{Q}}\right], \tag{46}$$

then there are only two parameters that are thrown up, namely $\varepsilon k^{-3/2}$ and $\varepsilon^{-1}k^{-1/2}$. In his study Bogolepov [26] reduced the number of free parameters in the problem to just one by choosing ε so that

$$\varepsilon k^{-3/2} = \varepsilon^{-1}k^{-1/2} = R^* \quad \Rightarrow \quad \varepsilon = k^{1/2}, \quad R^* = k^{-1} \tag{47}$$

and referred to R^* as a Reynolds number: here we shall put $\varepsilon = 1$. Given these preliminary transformations of variables the stability equations (3a)–(3g) are written as a system in terms of $\widehat{\widehat{u}}$, $\widehat{\widehat{v}}$, $\widehat{\widehat{T}}$ and $\widehat{\widehat{Q}}$ as defined in (46). This set can be expressed as

$$\left\{\frac{d^2}{d\widehat{Y}^2}+a_u\frac{d}{d\widehat{Y}}-b_u\right\}\widehat{\widehat{u}}=r_{ut}\widehat{\widehat{T}}+r_{uv}\widehat{\widehat{v}}+d_{ut}\frac{d\widehat{\widehat{T}}}{d\widehat{Y}}, \tag{48a}$$

$$\left\{\frac{d^2}{d\widehat{Y}^2}+a_t\frac{d}{d\widehat{Y}}-b_t\right\}\widehat{\widehat{T}}=r_{tv}\widehat{\widehat{v}}, \tag{48b}$$

$$\left\{\frac{d^2}{d\widehat{Y}^2}+a_v\frac{d}{d\widehat{Y}}-b_v\right\}\widehat{\widehat{v}}=r_{vq}\widehat{\widehat{Q}}+r_{vt}\widehat{\widehat{T}}+d_{vt}\frac{d\widehat{\widehat{T}}}{d\widehat{Y}}, \tag{48c}$$

$$\left\{\frac{d^2}{d\widehat{Y}^2}+a_q\frac{d}{d\widehat{Y}}-b_q\right\}\widehat{\widehat{Q}}=r_{qu}\widehat{\widehat{u}}+r_{qv}\widehat{\widehat{v}}+r_{qt}\widehat{\widehat{T}}+d_{qt}\frac{d\widehat{\widehat{T}}}{d\widehat{Y}}+d_{qv}\frac{d\widehat{\widehat{v}}}{d\widehat{Y}}, \tag{48d}$$

and the coefficients here (which are relegated to the appendix) can be written in terms of $\bar{\theta}$, $\bar{u}$ and $\bar{q}$ as given by (45). Finally, this system needs to be solved subject to the homogeneous conditions

$$\widehat{\widehat{u}}=\widehat{\widehat{v}}=\widehat{\widehat{v}}_{\widehat{Y}}=\widehat{\widehat{T}}=0 \quad \text{at } \widehat{Y}=0 \text{ and as } \widehat{Y}\to\infty. \tag{49}$$

7. Numerical and asymptotic solutions of system

The disturbance equations (48) (subject to the boundary conditions (49)) were solved numerically by use of a finite-difference formulation similar to that proposed by Malik, Chuang and Hussaini [31]. In this, derivatives are replaced by second order accurate central-differences on a non-uniform mesh which leaves a block tri-diagonal algebraic system to invert of the form

$$A_j\phi_{j-1}+B_j\phi_j+C_j\phi_{j+1}=0, \quad j=2,\ldots,N, \tag{50}$$

where A_j, B_j and C_j are 4×4 matrices and $\phi_j=(U_j,T_j,V_j,Q_j)^{\mathrm{T}}$ is the solution vector where $U_j=\widehat{\widehat{u}}(\widehat{Y}_j)$, etc. The outer boundary conditions were imposed simply by setting $U_{N+1}=T_{N+1}=V_{N+1}=Q_{N+1}=0$ while the constraints on $\widehat{Y}=0$ were applied by putting $U_1=V_1=T_1=0$ and the final constraint followed after a suitable normalisation of the problem. Iteration on the growth rate parameter ensured that $\widehat{\widehat{v}}_{\widehat{Y}}=0$ at $\widehat{Y}=0$ and thereby eigensolutions of (48) identified. Finally, in order to inspect the properties of solutions in the physically sensible context, our results were expressed in terms of the dimensionless variables denoted with a subscript D in the previous section, see (40), rather than the variables of (48) which have been scaled on the wavenumber according to (44).

We begin our account of the strongly cooled modes with *figure 10* which illustrates some typical stationary solutions of (48). The dependence of the spatial growth rate parameter β_D is shown as a function of vortex wavenumber k for a selection of scaled wall temperatures in the range $0.1\leqslant T_{Dw}\leqslant 10$; within the wavenumber regime there is a local maximum in the growth rate and a neutrally stable mode. Also shown are the growth rates for the first six modes for a fixed wall temperature $T_{Dw}=1$. As would be expected, the higher modes are unstable over a decreasing band of wavenumbers—in fact further computations showed that for these higher modes the neutral values of k are remarkably insensitive to T_{Dw}. We also note that *figures 10(a)* and *10(b)* compare well with figures 1 and 4 respectively of Bogolepov [26] once differences in notation have been accounted for.

Next we consider some non-stationary solutions. It is evident from the definition (45) that when $\Omega_D=0$ all the coefficients in system (48) are real and solutions have purely real values of β_D. However once we are in the non-stationary case this no longer holds and *figure 11* shows the dependences of the neutral values

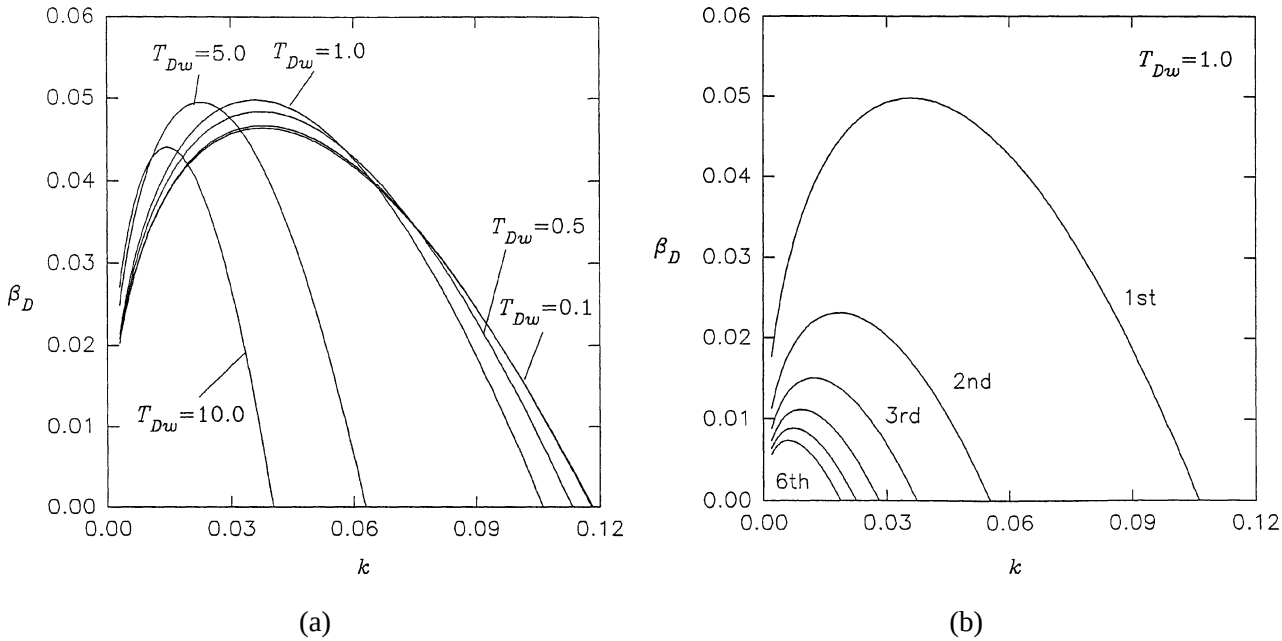

Figure 10. (a) Growth rate β_D of severely cooled modes as a function of wavenumber k for a selection of cooling parameters $0.1 \leqslant T_{Dw} \leqslant 10$. (b) Growth rates of first six severely cooled modes for fixed wall temperature $T_{Dw} = 1$.

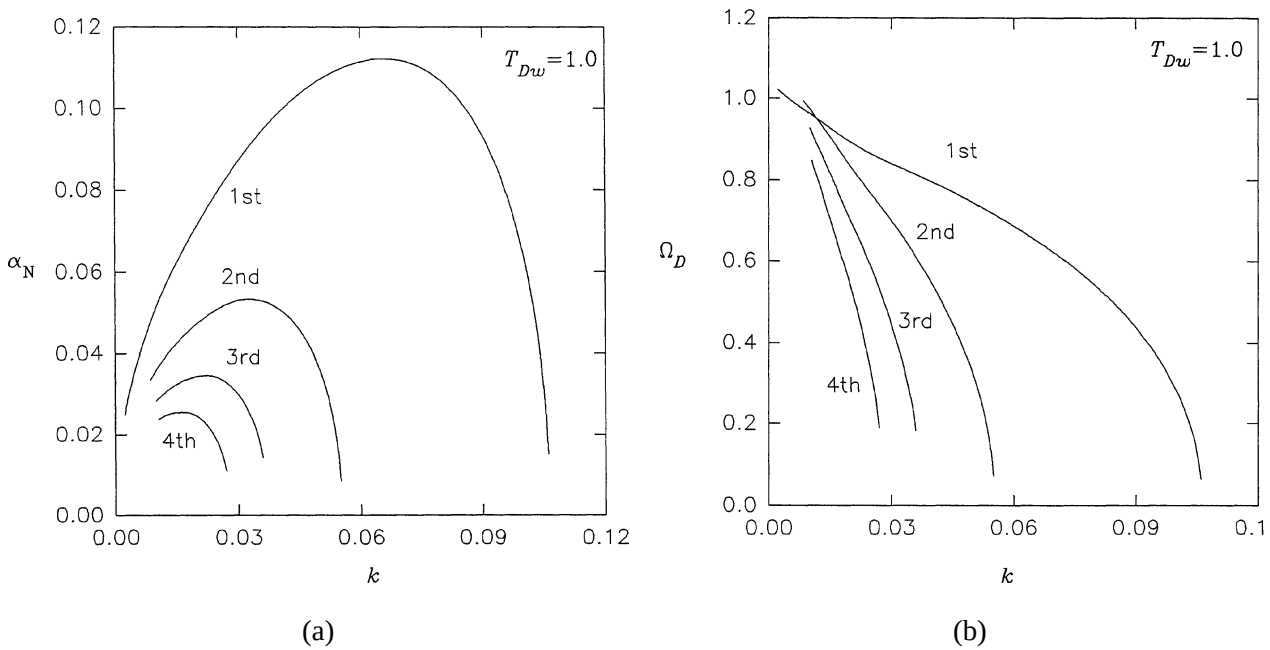

Figure 11. First four non-stationary severely cooled neutral modes at wall temperature $T_{Dw} = 1$. (a) $\alpha_N \equiv \mathrm{Im}(\beta_D)$ and (b) frequency Ω_D as functions of vortex wavenumber k.

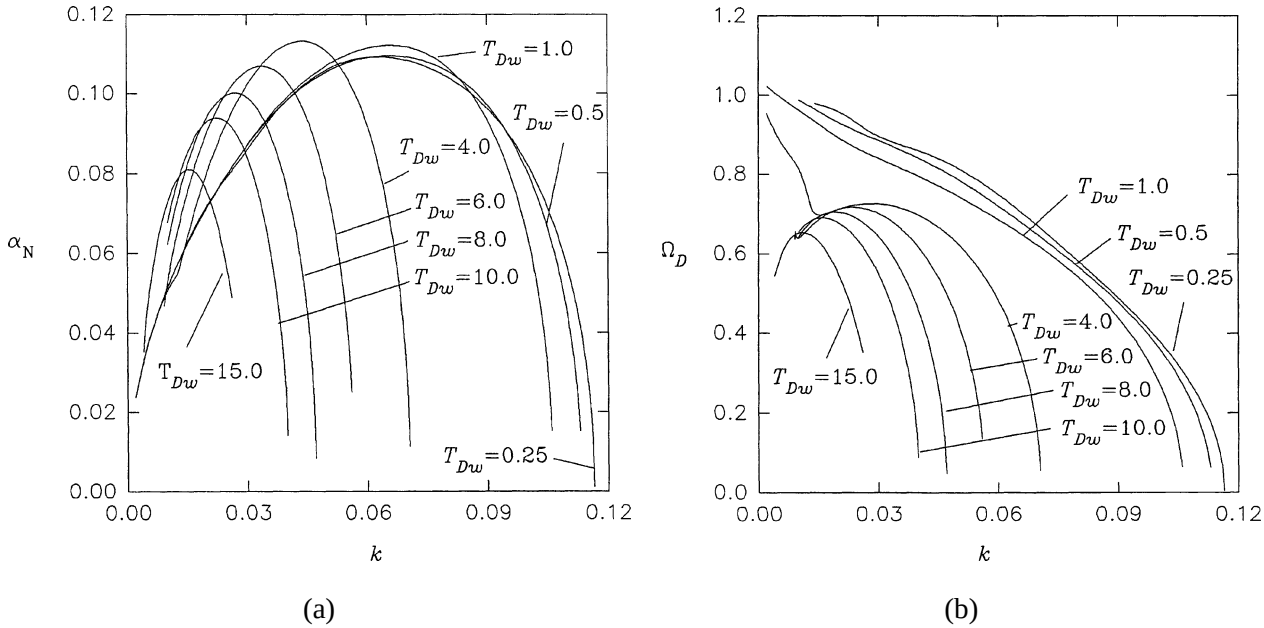

Figure 12. Properties of neutrally stable non-stationary modes in flows over a surface with prescribed wall temperature in the range $0.25 \leqslant T_{Dw} \leqslant 15$. (a) $\alpha_N \equiv \mathrm{Im}(\beta_D)$ and (b) frequency Ω_D as functions of vortex wavenumber k.

$\alpha_N \equiv \mathrm{Im}(\beta_D)$ and of Ω_D upon the wavenumber k for a fixed wall temperature $T_{Dw} = 1$. Of course, as $\Omega_D \to 0$ we retrieve the neutral stationary results which match with those of *figure 10(b)* but, of more interest, is the finding that $\Omega_D \to \infty$ in the long wavelength limit $k \to 0$. The properties of neutral modes as functions of k are shown in *figure 12*. In particular we notice that for smallish k the corresponding neutral α_N appears to be virtually independent of the wall temperature. Once more there appears to be a diversity in the behaviour of the frequency Ω_D in the small wavenumber limit: for very strong wall cooling $T_{Dw} \ll 1$, $\Omega_D \to \infty$ in this limit while, at higher T_{Dw}, $\Omega_D \to 0$.

It is clear that there is a rich and varied structure to the severely cooled stage. Interesting properties of these modes include both non-uniqueness and multiplicity of modes. Space precludes us from presenting many of the results but, as the main focus in this work has been the determination of new cooled structures and the linkages between them, in *figure 13* we summarise the neutral properties of non-stationary modes as functions of T_{Dw} for given values of the ratio k/α_N^2. It is observed that for $k/\alpha_N^2 < 4$ we appear to have two branches of solutions while only one otherwise. (Indeed at small values of the temperature there were problem in obtaining satisfactory convergence for those solutions without a second branch.) As an attempt to explain these findings it is clear that one branch represents the match with the moderately cooled modes found earlier (see Section 7.1 below) while the appearance of the second branch suggests that there is a possibility that the neutral curve closes up, especially since in limits with k/α_N^2 held fixed these severely cooled modes can be linked not only to the moderately cooled modes but also with the non-stationary counterparts to the viscous modes II and inviscid modes III of *figure 1*. Further calculations show that the higher modes behave in a very similar way.

7.1. Limiting forms of solutions

Two natural limits arise from these severely cooled calculations: these are both concerned with the case of $\widehat{T}_w \propto T_{Dw}$ large and $k \ll 1$. The first of these relates to the situation of large or O(1) values of the scaled

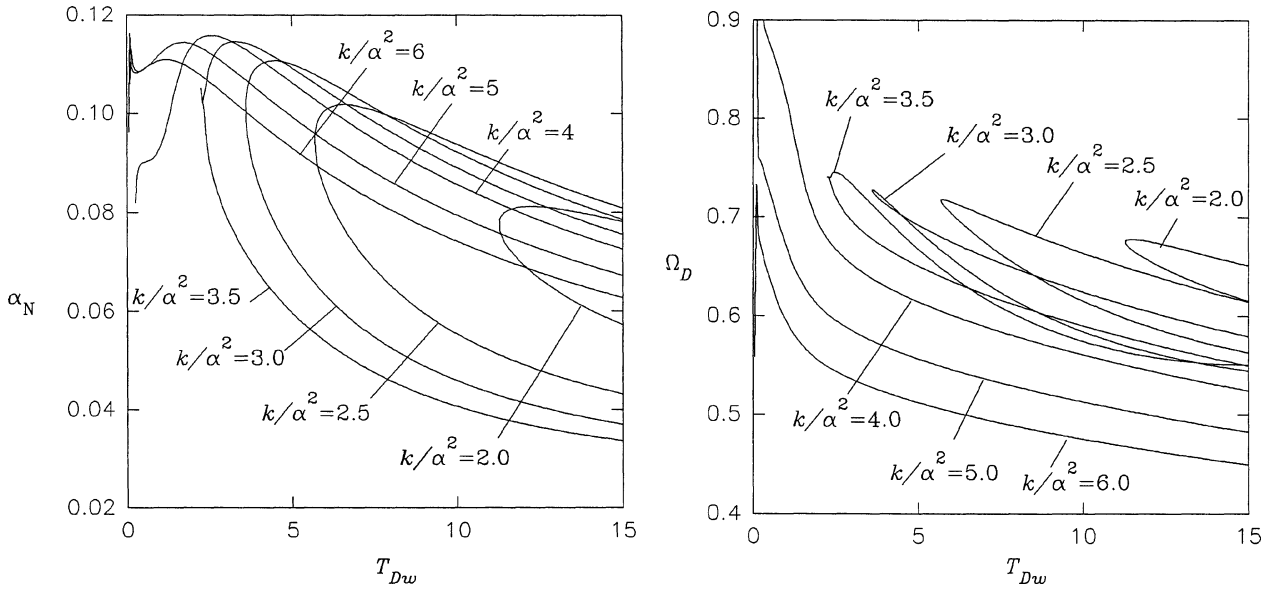

Figure 13. Neutrally stable non-stationary modes with prescribed k/α_N^2. (a) $\alpha_N \equiv \mathrm{Im}(\beta_D)$ and (b) frequency Ω_D as functions of wall temperature T_{Dw}.

temperature $\tau = k^{1/2} T_{Dw}$. We have already touched on this aspect when it was noted that the three regimes I–III in incompressible flow fall onto the same single structure when $S_w = \mathrm{O}(T_w^{-1/4})$ and $M_\infty = \mathrm{O}(1)$. To retrieve structures I–III from equations (48) is an elementary, though lengthy, task. Essentially all the key scalings are already held within (32)–(34) so that for $\widehat{T}_w \gg 1$ (see (36)) the necessary behaviours of the various quantities in (48) can almost be read off. As an example, in order to match to the inviscid mode examined by Dando [27] in the compressible regime, the relevant scalings for $\widehat{v}$, $\widehat{w}$ and $\widehat{p}$ within (37c) are $\mathrm{O}(\widehat{T}_w)$, $\mathrm{O}(\widehat{T}_w)$ and $\mathrm{O}(\widehat{T}_w^2)$ which are seen to be just the exponents of the S_w terms in (34b). The same recipe yields the appropriate behaviours for the growth rate β, spanwise wavenumber k and spatial extent Y of the mode for large $\widehat{T}_w$. For brevity we do not write out the full equations in this limit for these are essentially just the forms solved in previous calculations. Moreover, when $\widehat{T}_w$ formally reaches size $\mathrm{O}(G^{1/4})$ so the respective incompressible scalings are obtained and this provides the matching to the structures which were discussed in Section 3.

The second limit of this severely cooled work arises for small values of the scaled temperature τ and provides a link with the moderately cooled structures. When $\tau \ll 1$ the nature of the basic flow solution (45) indicates the evolution of two important spatial scales: a main region where $\widehat{Y} = \mathrm{O}(1)$ supplemented by a 'buffer layer' wherein $\widehat{Y} = \mathrm{O}(\tau^2)$. If we suppose that an additional viscous layer will be required in order to fulfill the no-slip conditions then, after noting that for $\widehat{Y} \ll \tau^2$, $\bar{\theta} \sim \tau$ (from (45)), the balance of the viscous and $b_u \widehat{u}$ terms in (48a) implies that within this third zone $\widehat{Y} \sim k^{1/2} \widehat{\beta}^{-1/3} \tau$, $\widehat{\Omega} \sim k^{1/2} \widehat{\beta}^{2/3}$. The results of the analysis of Denier et al. [8] and Dando and Seddougui [10] for inviscid Görtler vortices indicate that $\widehat{\beta} = \mathrm{O}(k^{1/2})$. If we assume this for the moment then the requirement that the viscous layer must lie beneath the buffer deck translates into the result that this main-buffer-viscous three layer structure may be possible as long as

$$k^{1/3} \ll \tau \ll 1. \tag{51}$$

To outline this further let us write

$$\widehat{\beta} = k^{1/2}\widetilde{\beta}, \qquad \widehat{\Omega} = k^{5/6}\widetilde{\Omega} \tag{52}$$

and take the three zones one at a time.

7.1.1. The buffer zone $\widehat{Y} = \mathrm{O}(\tau^2)$

If in the buffer layer $\widehat{Y} = \tau^2\overline{Y}$ then the basic flow solutions

$$\bar{\theta} = \tau\left[1 + 2\overline{Y}\right]^{1/2} \equiv \tau\overline{T}_0, \qquad \bar{u} = \tau\left[\left\{1 + 2\overline{Y}\right\}^{1/2} - 1\right] \equiv \tau\bar{u}_0$$

and scaling arguments applied to system (48) yield

$$(\widehat{\widehat{u}}, \widehat{\widehat{v}}, \widehat{\widehat{T}}, \widehat{\widehat{Q}}) = (U_0 + \cdots, k^{1/2}\tau^2 V_0 + \cdots, T_0 + \cdots, k^{1/2}\tau^{-2}Q_0 + \cdots). \tag{53}$$

Elementary analysis then leads to

$$U_0 = (A + BF)\bar{u}_0', \tag{54}$$

where A and B are constants and $F' = -\overline{T}_0/\bar{u}_0^2$ (here $'$ denotes $d/d\overline{Y}$).

7.1.2. The wall layer $\widehat{Y} = \mathrm{O}(k^{1/3}\tau)$

Within the wall layer we suppose that $\widehat{Y} = k^{1/3}\tau\widetilde{y}$, $\widetilde{y} = \mathrm{O}(1)$ and remark that the solutions of the buffer layer problem imply that within this viscous wall layer the disturbance functions in (48) assume the forms

$$(\widehat{\widehat{u}}, \widehat{\widehat{v}}, \widehat{\widehat{T}}, \widehat{\widehat{Q}}) = (\widetilde{u}_0 + \cdots, k^{5/6}\tau\widetilde{v}_0 + \cdots, \widetilde{T}_0 + \cdots, k^{1/6}\tau^{-1}\widetilde{Q}_0 + \cdots). \tag{55}$$

The governing equations must be solved subject to no-slip conditions on $\widetilde{y} = 0$ and matching with the buffer layer forms as $\widetilde{y} \to \infty$ and standard procedures show this is only possible if

$$\frac{B\tau}{Ak^{1/3}} = \frac{\mathrm{Ai}'(\xi_0)}{\widetilde{\beta}^{1/3}}\left\{\int_{\xi_0}^{\infty}\mathrm{Ai}(s)\,ds\right\}^{-1}, \tag{56}$$

where $\xi_0 \equiv -i\widetilde{\Omega}/\widetilde{\beta}^{2/3}$.

7.1.3. The main deck $\widehat{Y} = \mathrm{O}(1)$

To complete the description of this new structure it is necessary to consider the uppermost of the three tiers. The buffer deck solutions imply that within the main layer

$$(\widehat{\widehat{u}}, \widehat{\widehat{v}}, \widehat{\widehat{T}}, \widehat{\widehat{Q}}) = \tau(\widehat{U}_0^{\dagger} + \cdots, k^{1/2}\widehat{V}_0^{\dagger} + \cdots, \widehat{T}_0^{\dagger} + \cdots, k^{1/2}\widehat{Q}_0^{\dagger} + \cdots) \tag{57}$$

and then equations (48) may be used to show that

$$\widehat{Y}\frac{d^2\widehat{U}_0^{\dagger}}{d\widehat{Y}^2} + \frac{3}{2}\frac{d\widehat{U}_0^{\dagger}}{d\widehat{Y}} - \left[\widehat{Y} - \frac{1}{4\widetilde{\beta}^2}\right]\widehat{U}_0^{\dagger} = 0. \tag{58}$$

The relevant solution of this equation which both matches to the buffer layer as $\widehat{Y} \to 0$ and which decays as $\widehat{Y} \to \infty$ can take on one of two forms depending on the relative sizes of the constants A and B in (54). First, if

$B/A \ll \tau$, which from (56) corresponds to the regime $\tau \gg k^{1/6}$, we have effectively an inviscid analysis. The leading order solution is then

$$\widetilde{\beta} = (1/2)^{1/2}, \tag{59a}$$

$$\widehat{U}_0^{\dagger} \propto \widehat{Y}^{-1/2} \exp(-\widehat{Y}) \tag{59b}$$

which contrasts with the non-singular form obtained by Bogolepov [26] from a similar inviscid analysis. Alternatively, if $B/A = \mathrm{O}(\tau)$ we obtain

$$\widehat{U}_0^{\dagger} \propto \widehat{Y}^{-1/2} \exp(-\widehat{Y}) U\left(a; \tfrac{1}{2}; 2\widehat{Y}\right);$$

here $a \equiv 1/4 - (1/8)\widetilde{\beta}^{-2}$ and $U(a; 1/2; 2\widehat{Y})$ is the confluent hypergeometric function which is only algebraically large for $\widehat{Y} \gg 1$, see Abramowitz and Stegun [28]. Matching with the buffer deck solution, followed by use of (56), throws up the dispersion relation

$$\frac{1}{p^2 \widetilde{\beta}^{1/3}} \frac{\mathrm{Ai}'(\xi_0)}{\int_{\xi_0}^{\infty} \mathrm{Ai}(s)\, ds} = \frac{2\Gamma((1/2)+a)}{\Gamma(a)}; \tag{60}$$

here p is the order one parameter given by $p \equiv \tau k^{-1/6} \propto \widehat{T}_w k^{1/3}$. This result holds good so long as $\widehat{T}_w = \mathrm{O}(k^{-1/3}) \gg 1$ or, equivalently $\tau = \mathrm{O}(k^{1/6}) \ll 1$, which is within the range of validity as specified by (51).

It is of interest to note that if k is decreased to be $\mathrm{O}(G^{-1/2})$ then $\widehat{\beta} = \mathrm{O}(G^{-1/4})$ and the overall vortex wavenumber and spatial growth rate become $\mathrm{O}(1)$ and $\mathrm{O}(G^{1/2})$ respectively (see (37)). Then $\tau = \mathrm{O}(G^{-1/12})$ and $\widehat{T}_w = \mathrm{O}(G^{1/6})$ and use of (36) and (40) show that the wall temperature $T_w = \mathrm{O}(G^{-1/12})$. These new scalings, which correspond to longer wavelengths and to less severe cooling of the wall, are no more than the moderately cooled scalings discussed in Section 4. Furthermore, a large wavenumber analysis of the moderately cooled equations in Section 4 also establishes the dispersion relation (60).

The eigenrelation (60) was solved numerically and in *figure 14(a)* we show the growth rate $\widetilde{\beta}_r$ as a function of p^{-1} for the case of stationary modes. Nonstationary counterparts of this mode are illustrated in *figure 14(b)* from which we deduce that as a general rule increasing the frequency tends to lower the growth rate. Further computations revealed the existence of a second family of unsteady vortices and the real and imaginary parts of $\widetilde{\beta}$ are plotted as functions of $\widetilde{\Omega}$ in *figures 14(c)* and *14(d)*. We remark on the excellent agreement with the overall structure of *figure 8* for small τ. Now for sufficiently large values of the parameter p there are neutral modes and *figures 14(e)* and *14(f)* show the forms of the neutral values of $\widetilde{\beta}_i$ and frequency. Once more there is very good agreement with the moderately cooled results presented in *figure 6*. This connection between a moderately cooled viscous–inviscid stage and a severe cooled fully viscous problem has been encountered in previous studies of wall cooling (although we also point out that no relevant numerical solutions of the fully viscous regime have been given elsewhere). Elliott and Strange [30] have demonstrated that similar relationships hold in the context of Tollmien–Schlichting waves in cooled boundary layer flows for which analogous inviscid and viscous regimes exist.

8. Discussion

The highlight of our work summarised here has undoubtedly been the identification of two new structures which are relevant to Görtler vortices in cooled boundary layer flows. In particular we have uncovered an interactive moderately cooled structure which is certainly novel with regard to Görtler vortices. In effect, this

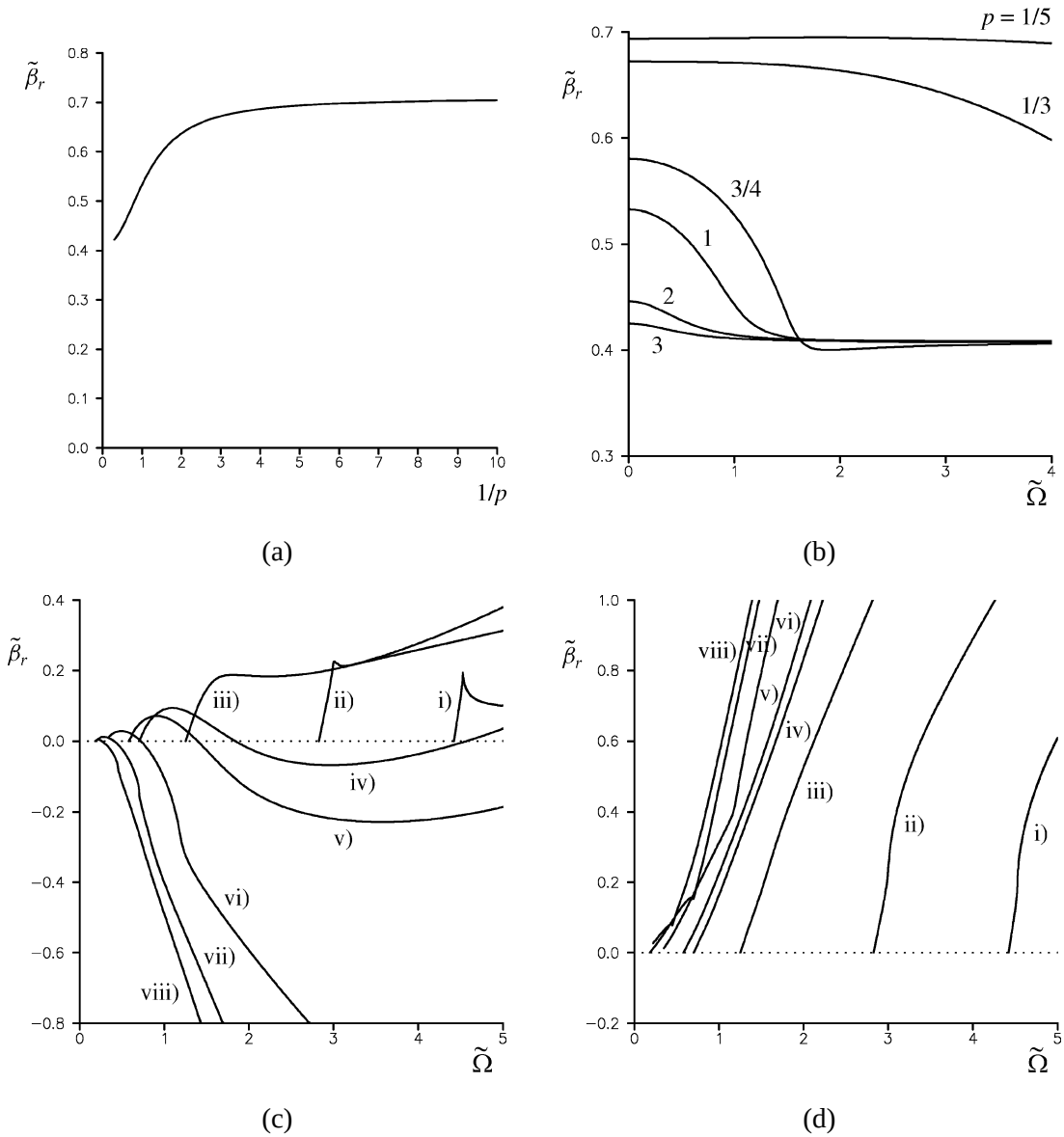

Figure 14. Solutions of the dispersion relation (60). (a) Stationary solutions: real part $\widetilde{\beta}_r$ of $\widetilde{\beta}$ as a function of parameter $1/p$. (b) Nonstationary solutions: $\widetilde{\beta}_r$ against frequency $\widetilde{\Omega}$ for various choices of p, $p = 1/5$ (topmost line), followed by $p = 1/3$, 3/4, 1, 2 and 3. (c) Real part $\widetilde{\beta}_r$ and (d) Imaginary part $\widetilde{\beta}_i$ plotted as functions of $\widetilde{\Omega}$ for a selection of values of p: the curves labelled (i)–(viii) correspond to $p = 2.5$, 2, 4/3, 1, 0.9, 2/3, 0.5 and 0.4 respectively. (e), (f) Dependences of $\widetilde{\beta}_i$ and $\widetilde{\Omega}$ on $1/p$ for neutral solutions.

mode combines the viscous study of CHS [14] and the inviscid modes of Seddougui et al. [19] into a single structure. Additionally, we have established the fully viscous form adopted by a severely cooled vortex, which is specifically new for $M_\infty = \mathrm{O}(1)$. This mode encapsulates the properties of the uncooled modes I–III of *figure 1* and unifies them: in particular there exists both a most unstable form and a right-hand branch for stationary modes within this parameter regime. Furthermore, the unsteady neutral calculations given in Section 7 for the plethora of possible modes demonstrates clearly the complexity of the structure. Obviously this needs to be investigated further.

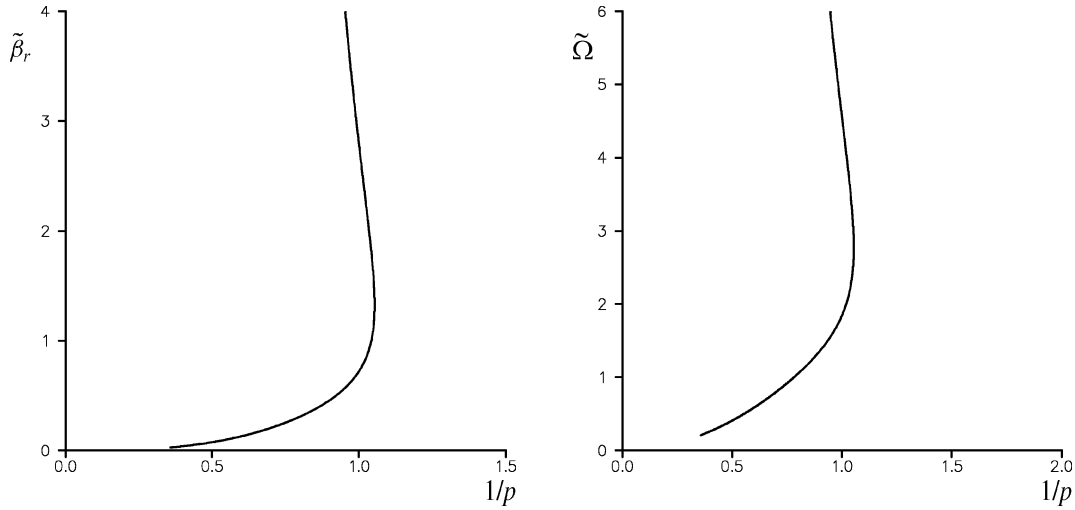

(e) (f)

Figure 14. (Continued.)

Unquestionably there are several limitations to our study but, on the other hand, a strong point is our identification of the links between the new cooled structures and the uncooled modes. In particular, Section 7.1 explains the connection between the moderately and severely cooled forms and while some of the trends are analogous to results of Seddougui et al. [19] with regards to cooled Tollmien–Schlichting waves, some are not. Our calculations, which in practice were far more extensive than the small selection presented here, clarify these links and, where direct comparison is possible with previous investigations, the agreement is very good.

We can summarise clearly how our novel modes relate to previously known forms and this information is presented in *figure 15*. In these diagrams—which are drawn for O(1) values of M_∞—we show the salient wall temperature/vortex wavenumber and T_w/growth rate regimes. Let us comment on *figure 15(a)*: a similar interpretation holds for the other diagram. For $T_w = \mathrm{O}(1)$ we have the four mode types I–IV described in the introduction from the right hand neutral branch I of Hall [4] down to the long wavelength interactive vortices IV obtained by CHS [14]. As the wall is gradually cooled so it is the long wavelength modes which are the first to be significantly affected. Cooling has the effect of enhancing the growth rates of these modes (see *figure 15(b)*) to rival those of inviscid vortices (cf. the analogous result of Seddougui et al. [19] in the context of Tollmien–Schlichting waves). Once $T_w = \mathrm{O}(G^{-1/12})$ the modes I, III and IV of *figure 1* collapse onto the moderately cooled, predominantly inviscid forms as described in Section 4. As T_w is reduced further, the modes I–III unite as a common fully viscous structure—that is our severely cooled mode of Sections 6 and 7.

The principal conclusion to be drawn from our studies is that cooling is destabilising for Görtler modes and *figure 15(b)* demonstrates that it is the severely cooled family of vortices which have the greatest growth rates. This destabilising effect of cooling is consistent with the conclusions drawn by El Hady [18] and Bogolepov [26] as a result of their numerical studies. Some of the calculations described in Section 7 suggest that should the wall temperature be less than $\mathrm{O}(G^{-1/12})$ then growth rates diminish once more: one would then anticipate that with enough cooling the boundary layer could be rendered stable to all wavelength vortices.

One limitation of our work is that we have been able to report on relatively few calculations and a more comprehensive description of effects like unsteadiness or the imposition of crossflow might have been contemplated. In the course of our studies here we have examined the influence of crossflow but, in the interests

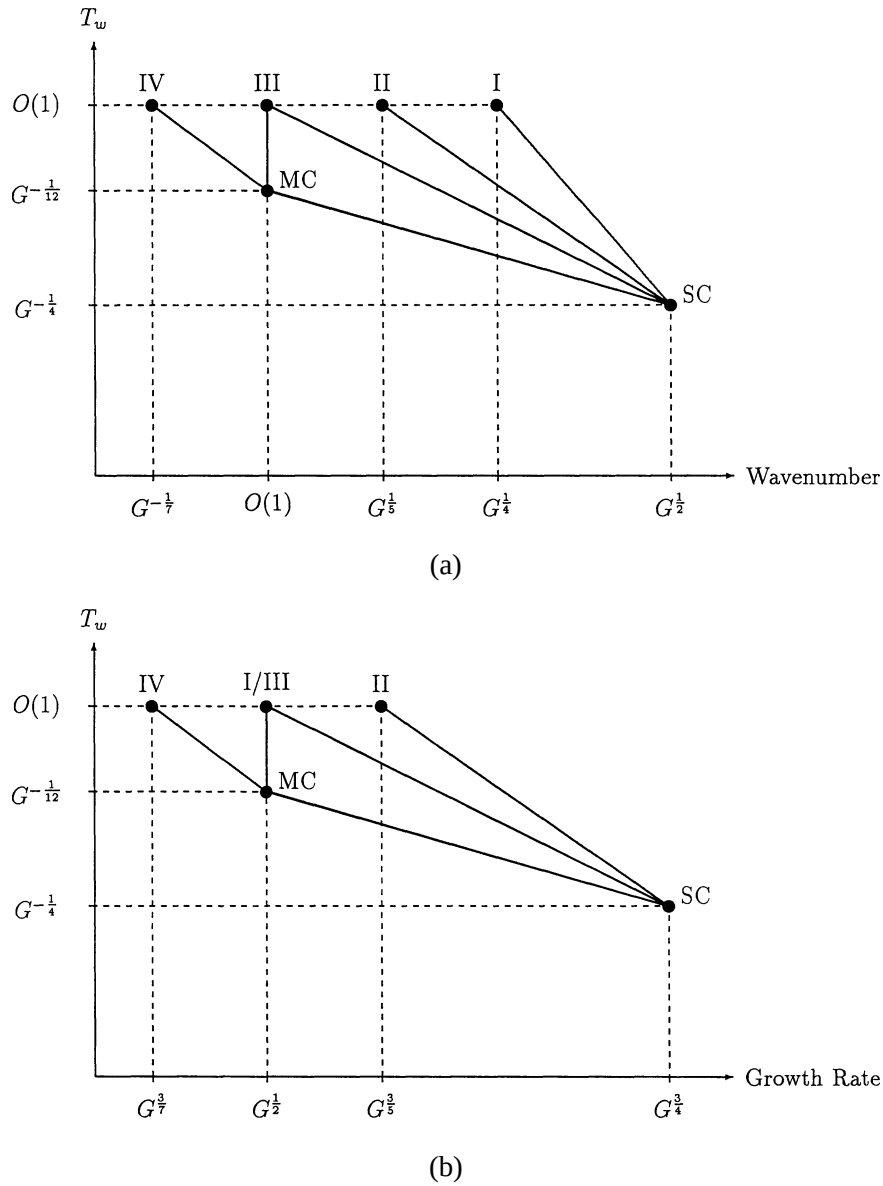

Figure 15. Diagrams in (a) wall temperature/vortex wavenumber space and (b) in wall temperature/growth rate space showing relationships between the uncooled modes and the new moderately cooled (MC) and severely cooled (SC) structures.

of conciseness, we defer discussion of this to elsewhere. However, it is worth remarking that an important conclusion which has arisen from our crossflow considerations is that it has no effect on the growth rates of the severely cooled modes. Thus, in particular, it does not lead to stabilisation as is often the case. Hence we may tentatively conclude that if cooling is applied to a fully three-dimensional boundary layer, which is often thought to be a method for protecting the flow from instability, it may actually make the boundary layer more susceptible to breakdown via Görtler modes. The lack of corroborative experimental evidence means that at this stage this prediction must remain somewhat speculative but our findings suggest that careful experimental studies of the effects of cooling on the properties of Görtler vortices would be of benefit.

From a theoretical viewpoint the introduction of unsteadiness and/or crossflow inevitably leads to critical layer type structures. Depending on the exact parameter scalings at hand, these critical layers could lie below, within or above the cooled sublayer of the basic flow and there clearly is ample scope for further developments here. The other aspect of this study which deserves further consideration is the form of the interactive dispersion relationship obtained by CHS [14] appropriate to a convex (rather than a concave) surface. In many respects this form when $\chi < 0$ behaves in a similar way to the eigenrelation which governs Tollmien–Schlichting modes and, in particular, in a high frequency limit one can identify a possible cooled 'upper branch' limit for which the wall temperature $T_w = \mathrm{O}(G^{-1/16})$ and the vortices are of wavenumber O(1) and frequency $\mathrm{O}(G^{-3/8})$. This corresponds to a weaker cooling than for the 'moderate' scales discussed in Section 4 but the problem that needs to be solved has some similarities with that tackled in Section 5. If we use the properties of upper-branch TS waves as elucidated by Elliott and Strange [30] as an analogy, it should prove possible to link this upper-branch-like vortex configuration to both the uncooled and severely cooled formulations. In the TS problem this type of argument led to the conclusion that within the severely cooled regime the neutral stability curve closes up and we intend to investigate whether similar behaviour occurs in the Görtler case. However what we believe we have presented here is some conclusive proof as to the significant part wall cooling can play in affecting the susceptibility of curved boundary-layer flows to the Görtler process.

Appendix

The coefficients of the various terms of the severely cooled equations (48) are given in terms of $\bar\theta$, $\bar u$ and $\bar q$ (see (45)) according to:

$$a_u = \bar\theta^{-1}\bar\theta', \qquad a_t = 2a_u, \qquad a_v = -\bar\theta^{-1}\bar\theta', \qquad a_q = a_t, \tag{61a–d}$$

$$b_u = 1 + \bar q k^{-3/2}\bar\theta^{-2}, \qquad b_v = 1 + \bar\theta^{-1}\left[\bar\theta'' - \bar\theta^{-1}\{\bar\theta'\}^2\right], \tag{61e,f}$$

$$b_t = 1 + \sigma\bar q k^{-3/2}\bar\theta^{-2} - \bar\theta^{-1}\bar\theta'', \qquad b_q = 1 + \bar q k^{-3/2}\bar\theta^{-2} - \bar\theta^{-1}\bar\theta'' \tag{61g,h}$$

and

$$r_{uv} = k^{-3/2}\bar\theta^{-2}\bar u', \qquad d_{ut} = -\bar\theta^{-1}\bar u', \qquad r_{ut} = -\bar\theta^{-1}\bar u'', \tag{62a–c}$$

$$r_{tv} = \sigma k^{-3/2}\bar\theta^{-2)}\bar\theta', \qquad r_{vq} = 1, \qquad d_{qt} = \bar q\bar\theta^{-1}, \qquad r_{qt} = \bar\theta^{-1}\{\bar q' - \bar q\bar\theta^{-1}\bar\theta'\}, \tag{62d–g}$$

$$r_{qu} = -\bar u k^{-1/2}\bar\theta^{-2}, \qquad d_{qv} = \bar q k^{-\frac{3}{2}}\bar\theta^{-3}\bar\theta', \qquad d_{qt} = 2\bar\theta^{-1}\{\bar q'' - \bar\theta^{-1}\bar\theta'\bar q'\}, \tag{62h–j}$$

$$r_{qt} = \bar\theta^{-1}\left[\bar q''' - \bar q'\bar\theta^{-1}\bar\theta''\right] + 2\bar\theta^{-1}\{\bar q' - \bar q\bar\theta^{-1}\bar\theta'\} + \frac{1}{2}\bar u^2 k^{-1/2}\bar\theta^{-3} + \bar q k^{-3/2}\bar\theta^{-3}\{\bar q' - \bar q\bar\theta^{-1}\bar\theta' - \sigma\bar q'\}, \tag{62k}$$

$$r_{qv} = 2\bar\theta^{-1}\left\{\bar\theta'' + \bar\theta^{-1}(\bar\theta')^2\right\} + k^{-3/2}\bar\theta^{-2}\{\bar q'' - \bar q\bar\theta^{-2}(\bar\theta')^2 - \sigma\bar\theta^{-1}\bar\theta'\bar q'\}, \tag{62l}$$

where $'$ denotes differentiation with respect to $\widehat{Y}$.

Acknowledgements

The referees are thanked for numerous helpful comments which led to significant improvements in this work.

References

[1] Görtler H., Über eine dreidimensionale instabilität laminarer Grenzchichten an konkaven Wänden, NACA Tech. Memo. No. 1375, 1940.
[2] Hall P., The linear development of Görtler vortices in growing boundary layers, J. Fluid Mech. 130 (1983) 41–58.

[3] Wadey P.D., On the linear development of Görtler vortices in compressible boundary layers, Eur. J. Mech. B-Fluid. 11 (1992) 705–717.
[4] Hall P., Taylor–Görtler vortices in fully developed or boundary layer flows, J. Fluid Mech. 124 (1982) 475–494.
[5] Hall P., Görtler vortices in growing boundary layers: the leading edge receptivity problem, linear growth and the nonlinear breakdown stage, Mathematika 37 (1990) 151–189.
[6] Saric W.S., Görtler vortices, Ann. Rev. Fluid. Mech. 26 (1994) 379–409.
[7] Timoshin S.N., Asymptotic analysis of a spatially unstable Görtler vortex problem, Fluid Dynamics 25 (1990) 25–33.
[8] Denier J.P., Hall P., Seddougui S.O., On the receptivity problem for Görtler vortices—vortex motions induced by wall roughness, Philos. T. Roy. Soc. A 335 (1991) 51–85.
[9] Hall P., Malik M., The growth of Görtler vortices in compressible boundary layers, J. Eng. Math. 23 (1989) 239–251.
[10] Dando A.H., Seddougui S.O., The compressible Görtler problem in two-dimensional boundary layers, IMA J. Appl. Math. 51 (1993) 27–67.
[11] Rozhko S.B., Ruban A.I., Criss-cross interaction in three-dimensional boundary layers, Izv. Akad. Nauk SSSR, Mekh. Zhidk. Gaza 3 (1987) 42–50.
[12] Ruban A.I., Propagation of wave packets in the boundary layer on a curved surface, Izv. Akad. Nauk SSSR, Mekh. Zhidk. Gaza 2 (1990) 59–68.
[13] Rozhko S.B., Ruban A.I., Timoshin S.N., Interaction of the three-dimensional boundary layer with a stretched obstacle, Izv. Akad. Nauk SSSR, Mekh. Zhidk. Gaza 1 (1988) 39–48.
[14] Choudhari M., Hall P., Streett C., On spatial evolution of long-wavelength Görtler vortices governed by a viscous-inviscid interaction, Q. J. Mech. Appl. Math. 47 (1994) 207–229.
[15] Bogolepov V.V., Lipatov I.I., On the asymptotic theory of Görtler vortices in a boundary layer, Zh. Prikl. Mekh. i Tekh. Fiz. 3 (1992) 58–62.
[16] Mack L.M., On the inviscid acoustic-mode instability of supersonic shear flows. Part 1: Two-dimensional waves, Theor. Comput. Fluid Dyn. 2 (1990) 97–123.
[17] Shaw S., Duck P.W., The inviscid instability of supersonic flow past heated or cooled axisymmetric bodies, Phys. Fluids A-Fluid. 4 (1992) 1541–1557.
[18] El Hady N.M., Secondary instability of high-speed flows and the influence of wall cooling and suction, Phys. Fluids A-Fluid. 4 (1992) 727–743.
[19] Seddougui S.O., Bowles R.I., Smith F.T., Surface-cooling effects on compressible boundary-layer instability, and on upstream influence, Eur. J. Mech. B-Fluid. 10 (1991) 117–145.
[20] Brown S.N., Cheng H.K., Lee C.J., Inviscid-viscous interaction of triple-deck scales in a hypersonic flow with strong wall cooling, J. Fluid Mech. 220 (1990) 309–337.
[21] Kerimbekov R.M., Ruban A.I., Walker J.D., Hypersonic boundary-layer separation on a cold wall, J. Fluid Mech. 274 (1994) 163–195.
[22] El Hady N.M., Verma A.K., Instability of boundary layers along curved walls with suction or cooling, AIAA Paper No. 81-1010, 1981.
[23] Hall P., Fu Y., On the Görtler vortex instability mechanism at hypersonic speeds, Theor. Comput. Fluid Dyn. 1 (1989) 125–134.
[24] Fu Y.B., Hall P., Effects of Görtler vortices, wall cooling and gas dissociation on the Rayleigh instability in a hypersonic boundary layer, J. Fluid Mech. 247 (1993) 503–525.
[25] Fu Y.B., Hall P., Crossflow effects on the growth of inviscid Görtler vortices in a hypersonic boundary layer, J. Fluid Mech. 276 (1994) 343–367.
[26] Bogolepov V.V., Investigation of surface temperature influence on Görtler vortices incipience, AIAA paper 95-2297, 1995.
[27] Dando A.H., The inviscid compressible Görtler problem in three-dimensional boundary layers, Theor. Comput. Fluid Dyn. 3 (1992) 253–265.
[28] Abramowitz M., Stegun I.A., A Handbook of Mathematical Functions, National Bureau of Standards, Frankfurt, 1964.
[29] Smith F.T., On the high Reynolds-number theory of laminar flows, IMA J. Appl. Math. 28 (1982) 207–281.
[30] Elliott J.W., Strange M.E., The effect of surface cooling on upper branch planar boundary-layer stability, School of Mathematics Report, Univ. of Hull, 1996,
[31] Mack L.M., Chuang S., Hussaini M.Y., Accurate numerical solution of the compressible linear stability equations, Z. Angew. Math. Phys. 33 (1982) 189–201.